架橋構造を有する分子認識ペプチドの
試験管内淘汰に関する研究

2014 年 3 月

埼玉大学大学院理工学研究科（博士後期課程）

理工学専攻（主指導教員　根本直人）

望月　佑樹

Table of contents

Chapter 1: Introduction

1-1. Peptide aptamer

Antibodies have been used as a general reagent for molecular recognition in life science fields. Since the 1990s, monoclonal antibodies have been developed as molecular targeting drugs to treat diseases, including cancers and inflammatory disorders [1,2]. Despite their advantages of high affinity, specificity, long *in vivo* half-life and generally low immunogenicity, antibodies have several drawbacks as a therapeutic class. They are relatively large proteins comprised of multiple polypeptide chains, thus they are often costly to produce, unsuitable for intracellular targets, have poor tissue penetration, exhibit relatively low thermal stability and site-specific modifications of antibodies are difficult [3]. In addition, these characteristics may restrict the application of antibodies to other fields such as nanotechnology.

To circumvent these potential drawbacks, several types of alternative protein scaffolds have been developed [3-6] (Figure 1–1). The peptide aptamer consists of a short variable peptide domain presented in the context of a supporting protein scaffold [7,8], which is an alternative protein scaffold. In the first report of a peptide aptamer, a combinatorial library of constrained 20-residue peptides displayed by the active-site loop of *Escherichia coli* thioredoxin was used [9]. As mentioned above, other protein scaffolds with several variable peptide regions have also been investigated. Such protein scaffolds can be considered as an extension of peptide aptamers. Those

protein scaffolds can interact with targets via surfaces consisting of noncontiguous peptide sequences disseminated over several secondary structural elements or across several variable loops [4,5]. Although the number of randomized regions of these protein scaffolds is distinct from peptide aptamers, which have a single variable peptide region, the concept of constraining the peptide conformation using scaffold proteins can be considered a common feature of these affinity proteins.

Some groups have recently used peptides themselves as an affinity reagent as an alternative to antibodies, and termed the peptides, which exhibit affinity and specificity toward target molecules, as either ‘peptide aptamers’ or ‘peptide binders’ [10-12]. In this thesis, affinity reagents based on peptides will be indicated as ‘peptide aptamers’. Peptides can be chemically synthesized, thus facilitating the incorporation of several modifications to improve their properties. The peptide aptamers have been applied in several fields, for example in biology [13], material science [14] and medicine [15-17]. Currently, peptide binding to biomolecules as well as inorganic surfaces (metals, semiconductors and metal oxides) and organic molecules (nanocarbons, polymers and peptide assemblies) has been designed by an *in vitro* selection process [18-20]. Material-binding peptides with molecular-recognition and self-assembly capabilities represent new smart materials.

The molecular recognition ability of peptides towards several kinds of molecules/materials has been an attractive property. However, the use of peptides has several issues that need to be circumvented. Since peptides generally adopt random conformations, energetic and entropic

penalties upon binding to target molecules will be introduced [17]. Furthermore, peptides expose the vulnerable peptide bond to proteolytic attack, and finally undergo renal clearance. To overcome these deficiencies as an affinity reagent, several types of constrained peptides have been used as peptide aptamer candidates, e.g., cyclic peptide with a disulfide bond [21-23], bicyclic peptides with a chemical compound [21,24], non-natural amino-acid containing peptides [21,25] and disulfide-rich peptides [26-28]. Generally, these constrained peptides exhibit high-affinity and specificity towards target molecules and enhanced protease resistance when compared with their linear equivalents.

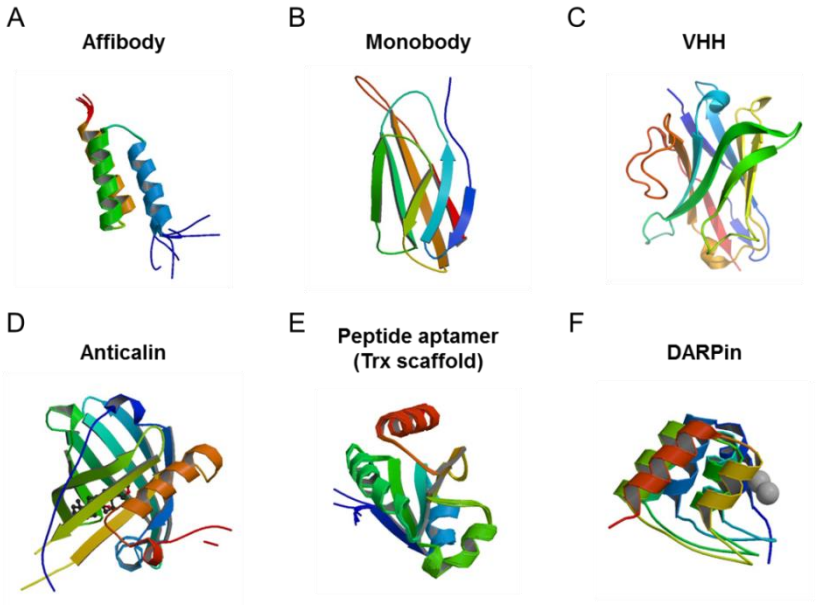

Figure 1–1. Representative protein display scaffolds. All images were obtained from PDB. (A) Affibody: Z-domain of protein A (2B88), (B) Monobody: 10th fibronectin type III domain (1TTG), (C) VHH: heavy-chain antibodies from camelids (1I3V), (D) Anticalin: lipocalin from human (1LNM), (E) Peptide aptamer: thioredoxin (Trx) scaffold (1XOB) (F) DARPin: designed ankyrin repeat proteins (1N0R).

1-2. Disulfide-rich peptides

Disulfide-rich peptides have been found in a wide variety of organisms and have exciting biological and medicinal applications owing to their stability and structure. Cystine knot peptides are a major class of disulfide-rich peptides, which have been isolated from various natural sources in animals and plants [29-31]. They are typically 30 amino acids in length and are defined by a common and extraordinarily stable tertiary fold (Figure 1–2). The first cysteine residue in the sequence is linked to the fourth residue, the second to the fifth and the third to the sixth. These three disulfide bridges endow cystine knot peptides with extraordinary proteolytic, thermal and chemical stability. They can be boiled, incubated at 65 °C for weeks, or even placed in 1 N HCl or 1 N NaOH, without loss of structural or functional integrity [32,33]. The loops between the successive cysteine residues of the cystine knot peptides are diversified with respect to length and amino acid composition, and thus the motif can be considered as a scaffold to display diverse bioactive peptide sequences. Given the above characteristics, cystine-knot peptides can be considered as promising drug candidates [34,35]. For example, conotoxins, isolated from the venom of marine cone snails, are potent and specific blockers of a variety of ion channels [36,37]. Indeed, the extensively studied MVIIA has been used clinically for the treatment of chronic pain [38]. On the other hand, cystine knot peptides can also be an attractive scaffold for the development of peptide-based diagnostics [39,40]. Kimura *et al.* reported that an engineered cystine-knot peptide that binds with high affinity

to integrin receptors can be used for tumor imaging by positron emission tomography [41].

Other than cystine knot peptides, three-finger (3F) peptides have been a highly attractive disulfide-rich peptide scaffold. 3F peptides have conserved residues that contribute to the characteristic fold. They include eight conserved cysteine residues found in the core region. In general, they are monomers that have minor differences in their loop lengths and the conformation of particular turns and twists [42]. Recently, it was reported that a new class of 3F peptides 'mambalgins' from the black mamba were able to abolish pain through inhibition of acid-sensing ion channels expressed in either central or peripheral neurons [43]. These peptides were not toxic in mice but showed a potent analgesic effect upon central and peripheral injection that can be as strong as morphine. This example may make three-finger peptides an attractive peptide-based drug candidate.

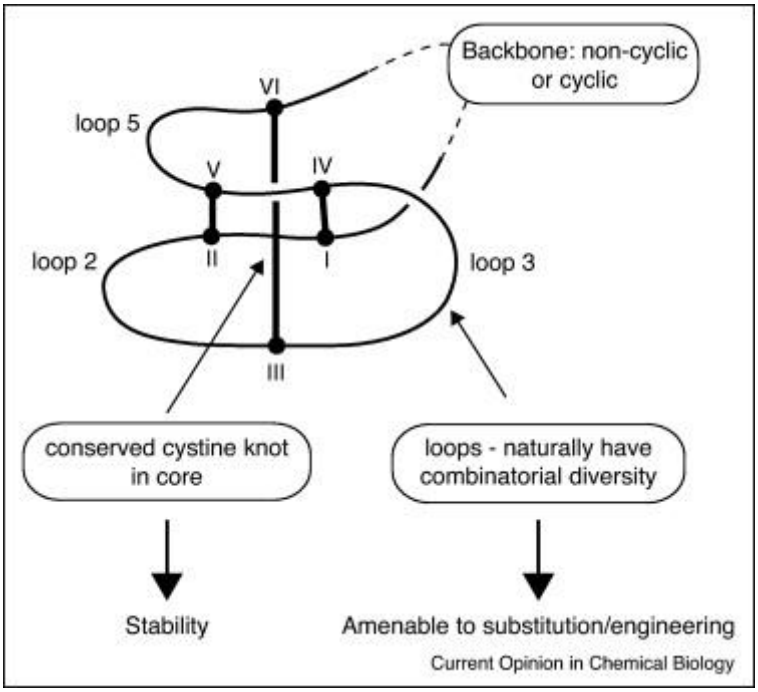

The material was obtained from Daly N.L. *et al.* [31].

Figure 1–2. The cystine knot motif. Inhibitor cystine knot and cyclic cystine knot (CCK) motifs are shown. The core of the motif consists from three disulfide bridges with I–IV, II–V and III–VI connectivity. The first two disulfide bridges form an embedded ring that is threaded by the III–VI disulfide bridge. Loop regions between successive cysteine residues have naturally occurring combinatorial diversity, which has led to cystine knot peptides being used as scaffold to display bioactive peptide. Backbone is cyclized in CCK which depicted by dished line.

1-3. *In vitro* display technologies

Directed evolution represents a powerful and well-established method to design the above affinity proteins or peptide aptamers [44,45]. Directed evolution mimics the process of natural selection to evolve proteins/peptides towards a desired function or set of properties, or even to generate proteins/peptides with novel functions. In protein evolution, since proteins cannot be amplified themselves, the linking of genotype (nucleic acid) to phenotype (protein/peptide) is required, which enables easy identification and amplification of the selected proteins via the DNA or RNA template. *In vitro* display technologies are virus-type strategies, in which the genotype and phenotype are physically connected. Over the past decade, several types of *in vitro* display technologies have been developed, as shown in Figures 1–3 [45,46].

One of the most commonly used *in vitro* display technologies is phage display, in which the protein of interest is displayed on the surface of the phage via coat proteins and the encoding DNA is encapsulated inside the phage. During the last decade, phage display has been widely used to select/evolve binding interactions, such as antibodies and alternative proteins scaffolds [45]. In addition, phage display has been used to select peptide aptamers from random peptide libraries [21-24]. Recently, selection of chemically modified peptides by phage display has been also reported [21]. However, phage display has several problems related to the use of living cells and bacteriophages themselves (e.g., small library size ($\approx 10^{10}$) limited by the transformation step, cell

toxicity of the displayed proteins and the effects of the fused coat proteins against function) [47].

To circumvent the above limitations, cell-independent *in vitro* display technologies using a cell-free translation system, such as ribosome display and mRNA display, have been developed [48-50]. In ribosome display, cell-free transcription and translation of a non-stop codon mRNA generates ternary complexes of mRNA, ribosome and the translated protein. No transformation of living cells is required, allowing generation of very large libraries of up to 10^{13} sequences. On the other hand, mRNA display involves the covalent puromycin linkage of RNA and protein, generating stable mRNA-protein fusions compared with ribosome display. Puromycin serves as a stable mimic of the 3'-region of amino-acyl tRNA. As it enters the ribosomal A site, it binds covalently to the C-terminus of nascent proteins as a result of the peptidyl transferase activity of the ribosome. However, in these technologies, the genotype is an RNA molecule, thus selection conditions are limited owing to the labile nature of RNA molecules. In addition, these methods appear to not be ‘‘user friendly’’, because they are used in a rather limited number of labs [44].

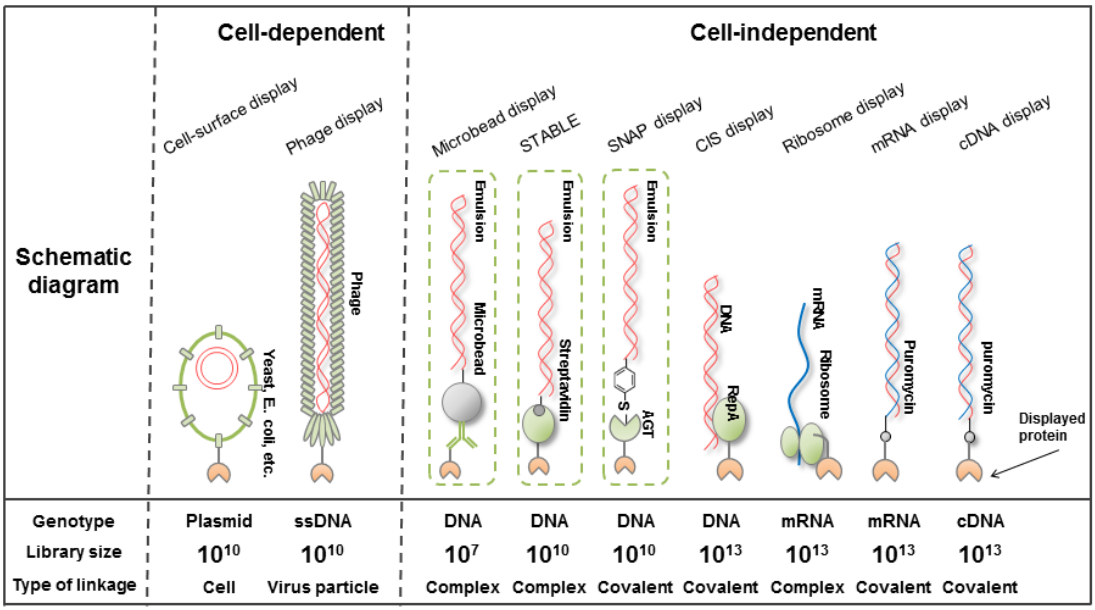

Figure 1–3. Schematic diagram of several types of virus type genotype-phenotype linking technologies.

1-4. cDNA display

To increase the stability of the mRNA display molecule, a puromycin-linker, which fuses a cDNA to a translated protein, was designed and is called cDNA display [51-53]. First, the designed puromycin-linker DNA (termed long biotin segment puromycin-linker (LBP-linker)) for cDNA display consists of a ‘ligation site’, a ‘biotin site’, a ‘reverse transcription primer site’ and a ‘restriction enzyme site’ (Figure 1–4A). cDNA is reverse transcribed from the primer site of the puromycin-linker DNA. Thus, the cDNA and the translated protein are covalently fused via the puromycin-linker DNA, which is a highly stable genotype-phenotype linkage. Then, to facilitate the cDNA display preparation, a simpler construct puromycin-linker DNA (named short biotin segment puromycin-linker (SBP-linker)), in which two G-ribonucleotides (rG) were incorporated as a replacement of the restriction enzyme site, was designed (Figure 1–4B) [54]. Furthermore, to extend the selection target varieties, modified puromycin-linker DNA in which the rGs were replaced with inosines was desogned [55].

Since the cDNA display molecule is highly stable and easily immobilized on a solid support via the biotin-streptavidin interaction, post-translational reactions such as the disulfide shuffling reaction can be easily performed. Thus, cDNA display method enable *in vitro* selection/evolution of disulfide-rich peptides (Figures 1–5). Indeed, *in vitro* evolutions of disulfide-rich peptide aptamers and three-finger peptides containing four disulfide bridges were

reported [52,56]. In addition, by taking advantage of the high stability of the cDNA display molecule, *in vitro* selection of a peptide aptamer against a receptor protein expressed on living cells was achieved [57]. Moreover, high affinity peptide aptamers were selected by the cDNA display method in combination with a technology that generates a huge diverse library using the Y-ligation-based block shuffling method [58]. As above, cDNA display method can be a powerful technology to design several kinds of peptide aptamers when compared with other *in vitro* display technologies.

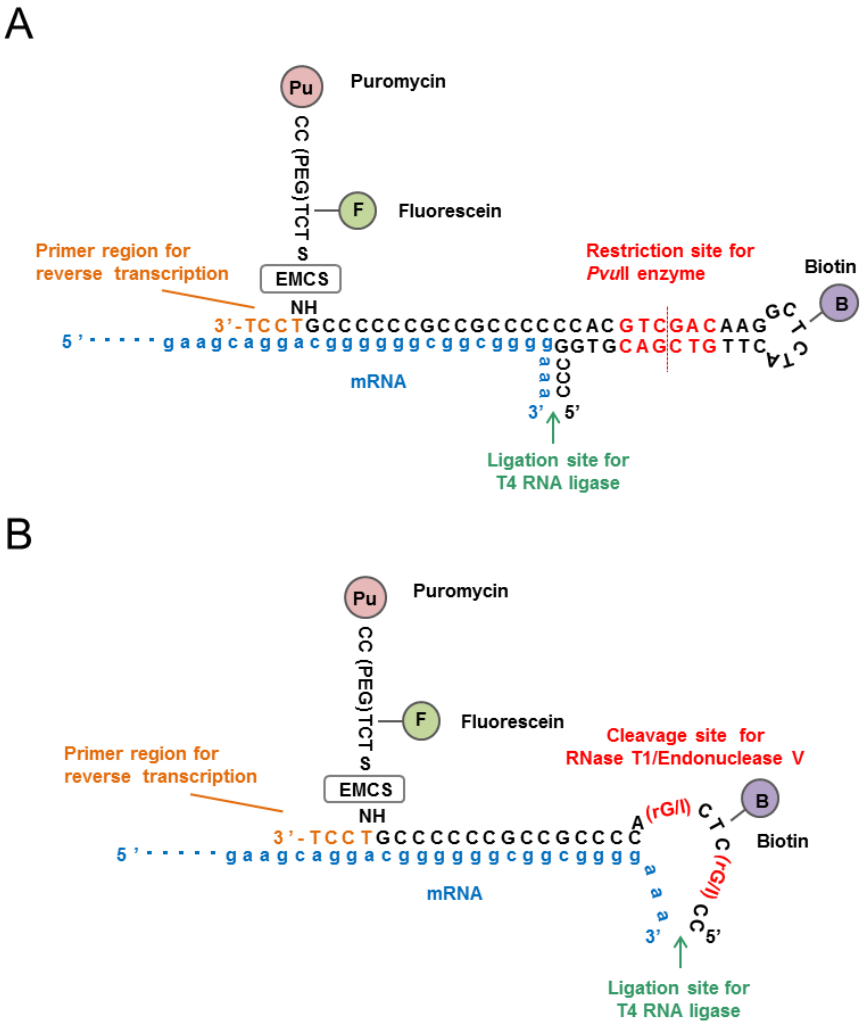

Figure 1–4. Schematic diagram of puromycin-linker DNAs for cDNA display. (A) Construct of LBP-linker. The LBP-linker construct comprises four parts: a ligation site for mRNA, a primer region for reverse transcription, a biotin moiety for the immobilization of the mRNA-linker conjugate on streptavidin-beads, and a restriction site for *Pvu*II enzyme to release the mRNA/cDNA-protein fusion molecule from the SA-beads. In addition, the LBP-linker includes puromycin (for the covalent linking of the expressed protein to mRNA) and fluorescein (for detection and quantification). The 3'-end of the mRNA is shown in lower case letters. [N-(6-maleimidcaproyloxy) succinimide] (EMCS) is bifunctional cross-linker used in the preparation of the LBP-linker. (B) Construct of SBP-linker. The SBP-linker has two cleavage sites for RNase T1 (G-ribonucleotide: rG) or endonuclease V (inosine: I) instead of the restriction site of LBP-linker.

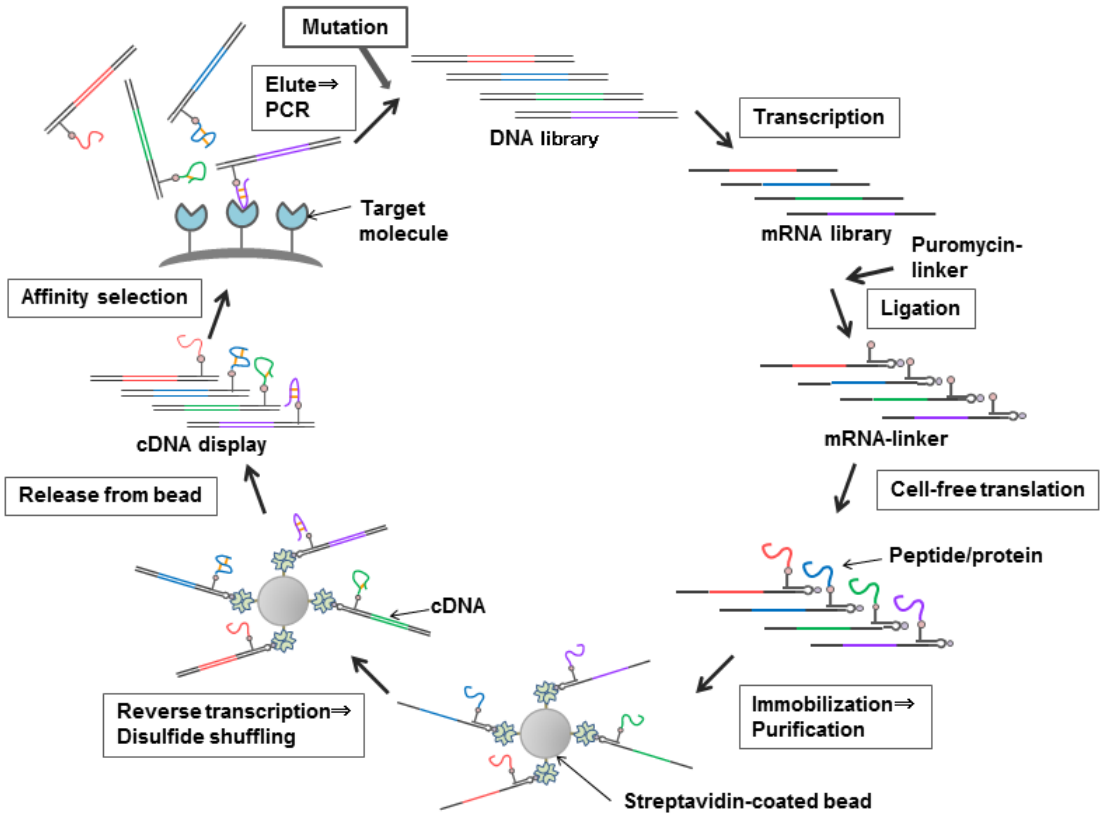

Figure 1–5. A schematic diagram of *in vitro* selection/evolution of disulfide-rich peptides by cDNA display method. DNA library coding disulfide-rich peptide is transcribed into mRNA and a puromycin-linker DNA is ligated to the 3'-terminus of the mRNA. mRNA-linker conjugates are translated with a cell-free translation system, resulting peptide-mRNA fusion molecules via a puromycin-linker DNA are synthesized. The peptide-mRNA fusions are immobilized on a streptavidin-coated bead using a biotin in the linker and reveres transcribed. After disulfide-shuffling reaction is performed, cDNA display molecules are released from the bead. Target binding cDNA display molecule is selected from the cDNA display molecule library and selected cDNA display molecule is amplified by PCR. Target binding disulfide-rich peptide is enriched by cycling above steps. By introducing mutations to the selected DNA during PCR amplification, disulfide-rich peptides can be evolved.

1-5. Aims of this study

As described in Chapter 1–3, as disulfide-rich peptides have attractive properties and functions they represent promising affinity reagents. A native disulfide-rich peptide-based library [41] and a library in which three cysteines were introduced at specific positions [59] were used. However *in vitro* selection/evolution of disulfide-rich peptides from a peptide library in which cysteines are randomly introduced has not been reported. The aim of this study was to establish an *in vitro* selection/evolution system by cDNA display method for disulfide-rich peptide aptamer design (Chapter 2) and create disulfide-rich peptide aptamers with unique functions (Chapter 3).

Chapter 2: Improvement of *in vitro* selection/evolution system by cDNA display method

2-1. Increasing the library size in cDNA display by optimizing purification procedures

2-1-1. Introduction

Although the cDNA display method have been useful for *in vitro* peptide and protein selection, its productivity was hindered by the generation of mRNA/cDNA-protein fusion molecules; only around 0.1% of the initial mRNA was ligated to proteins with a puromycin-linker [51]. Recently, this efficiency has been improved to more than 1% by introduction of a novel puromycin-linker and minor modification of previous method [52,54]. However, the yield of cDNA display fusion molecules is still smaller than that of mRNA display fusion molecules (20–30%). The aims of this study were to investigate which processes during the preparation of cDNA display fusion molecules shown in Figure 2–1 cause its low yield, and to increase the yield by overcoming these problems.

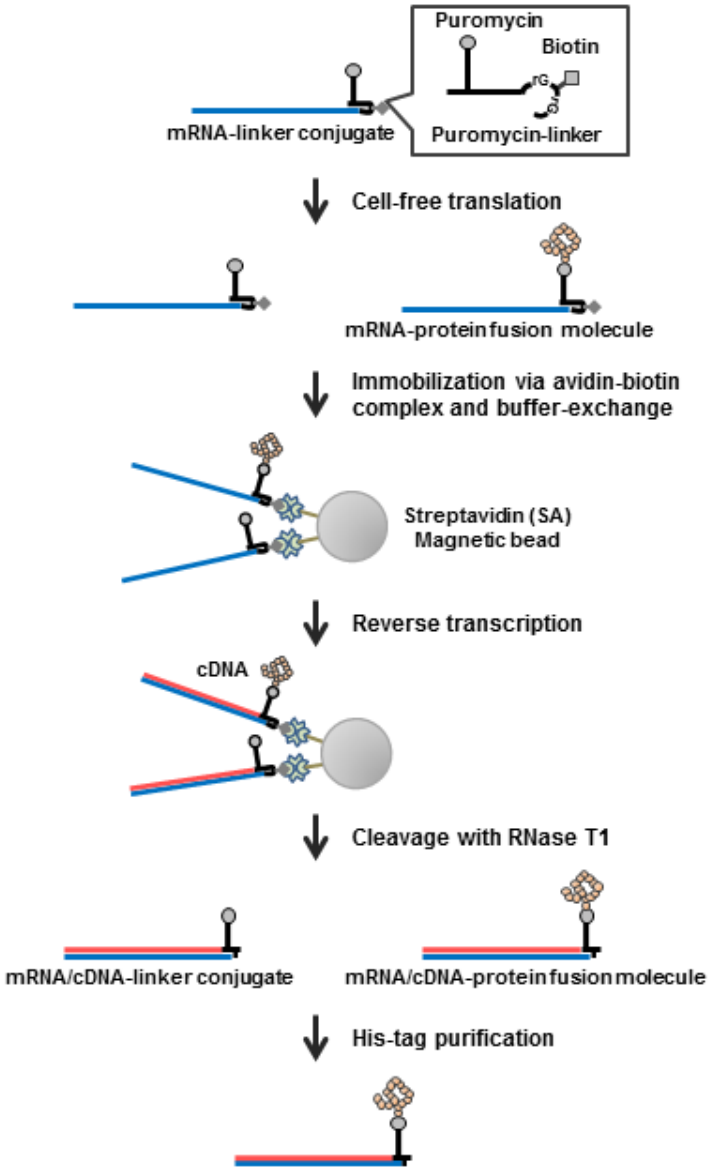

Figure 2–1. Scheme of cDNA display preparation. The mRNA-linker conjugate was prepared by ligation of a puromycin-linker DNA to the 3'-terminus of an mRNA coding B-domain of protein A (BDA). The mRNA-linker conjugate was translated by an *in vitro* translation reaction. The synthesized mRNA-protein fusion molecule and the remaining mRNA-linker conjugate were captured with SA-beads from the translation reaction mixture and reverse transcribed on the beads. The mRNA/cDNA-protein fusion molecule and the mRNA/cDNA molecule were released from the SA-beads by RNase T1 treatment. The mRNA/cDNA-protein fusion molecule was purified by the His-tag in the translated protein.

2-1-2. Materials and methods

DNAs coding B-domain of protein A were transcribed into mRNA using the T7 RiboMAX express large scale RNA production system (Promega, USA) and the synthesized mRNA purified with an RNA purification column (FavorPrep After Tri-Reagent RNA Clean-Up Kit, Favorgen, Taiwan). Puromycin-linker DNAs (1.2 μM) were hybridized to the purified mRNA (1 μM) under annealing conditions (heating to 90 °C for 2 min followed by incubation at 70 °C for 1 min, then cooling to 25 °C) in ligation buffer (50 mM Tris-HCl, pH 7.5, containing 10 mM $MgCl_2$, 10 mM dithiothreitol (DTT) and 1 mM ATP), then the 5'-terminus of the puromycin-linker DNA and the 3'-terminus of the mRNA were ligated with T4 RNA ligase (Takara Bio, Japan) and T4 polynucleotide kinase (T4 PNK; Toyobo, Japan) by incubation at 25 °C for 60 min.

Ligation products were translated in *in vitro* translation reaction solution (0.04 μM of ligated products) with the Retic Lysate IVT kit (Ambion, USA) by incubation at 30 °C for 20 min. Then, 3 M KCl and 1 M $MgCl_2$ were added to the reaction (final conc. of 900 mM, and 75 mM respectively) and incubated at 37 °C for 60 min. Further EDTA solution (0.5 M, pH 8.0) was added to the translation reaction (Final conc. of 92 mM) and incubated at 4 °C for 10 min. Then equal volume of 2X binding buffer (20 mM Tris-HCl, pH 7.5, 2 M NaCl, 2 mM EDTA, 0.1% Twenn-20) for streptavidin-coated magnetic beads (SA-beads, Dynabeads MyOne Streptavidin C1, Invitrogen, USA) was added to the EDTA-treated translation reaction mixture. 19.6 μL of the mixtures were

incubated with 0.75, 3.75, 10, or 20 μL of SA-beads at room temperature (r.t.) for 15 min. Then supernatants of each sample were subjected to 4% stacking–6% separating sodium dodecyl sulfate polyacrylamide gel electrophoresis (SDS-PAGE) containing 8 M urea.

Reverse transcription (RT) was performed at 40 °C for at least 10 min in 20 μL of the RT reaction mixture [50 mM Tris–HCl, pH 8.3, 75 mM KCl, 3 mM $MgCl_2$, 50 mM DTT, 0.5 mM dNTP mix and 200 U of SuperScriptIII reverse transcriptase (Invitrogen, USA)] . RNase T1 (10 U, Ambion, USA) and RNase H (10 U, Takara Bio, Japan) were added to the RT reaction mixture and incubated at 37 °C for 10 min. Released mRNA/cDNA-protein fusion molecules were confirmed by SDS-PAGE as the above.

2-1-3. Results and discussion

Firstly, the step collecting the mRNA-protein fusion molecules from the rabbit reticulocyte lysate was optimized. We speculated that ribosomes might strongly bind the mRNA-protein complex in the lysate before purification with SA-beads, which decrease the binding capacity of the SA-beads. Thus, we confirmed effect of EDTA treatment to release ribosomes against collecting efficiency of mRNA-protein fusion molecules from the translation mixture (Figure 2–2A, B). In addition, we found that SA-beads with a binding capacity 200 times the amount of biotinylated mRNA-protein

fusion molecules were required to purify almost the all fusion molecules (Figure 2–3A, B). Similarly, the final amount of purified cDNA-protein fusion molecules also increased with increased SA-beads (Figure 2–3C, D). These results suggest that steric hindrance might interfere with biotin-streptavidin binding considerably.

Second, we optimized the process from RNase T1 digestion to His-tag purification of cDNA display molecules shown in Figure 2–1. In the cDNA display method, it is very important to separate mRNA/cDNA-protein fusion molecules from mRNA/cDNA-linker conjugates (which are not fused with its coding proteins) to reduce the background in the in vitro selection. Thus His-tag sequence (His×6) was incorporated to the C-terminal region of a coding protein. In this study we examined whether RNase T1 can digest the guanine base of the SBP-linker in the His-tag-binding buffer containing imidazole. If possible, buffer exchange for His-tag purification after RNase T1 digestion would be eliminated and so there could be no loss of cDNA display molecules. We found that RNase T1 worked well in the His-tag-binding buffer, and cDNA-protein fusion molecules were efficiently purified by His-tag purification without any buffer exchanges (Figure 2–4A, B). As a result, this modification increased the yield of mRNA/cDNA-protein fusion molecules by 1.5 times over the previous method. Moreover, this improvement allows us to save time and cost in the preparation of mRNA/cDNA-protein fusion molecules and to help make cDNA display technology easier to use.

One of the crucial problems with cDNA display is the low yield of cDNA-protein fusion molecules, which is less than 1% of input mRNA-linker conjugates. In this thesis, we identified that the mRNA-ribosome-protein complex may sterically hinder the biotin-streptavidin interaction between the puromycin-linker DNA on the fusion molecules and the SA-beads. In addition, mRNA-protein fusion molecules without a ribosome could also interfere with the biotin-streptavidin interaction. Because of these reasons, more SA-beads than expected are required to purify most of the mRNA-protein fusion molecules. The addition of EDTA into the lysate after translation to remove the bound ribosome effectively increased the yield of cDNA display molecules. Furthermore, the simplification of His-tag purification after the release of cDNA display molecules from the SA-beads by performing RNase T1 digestion in the His-tag-binding buffer also increased the yield of cDNA display molecules. Finally we achieved 17% of final yield of cDNA display molecule based on the input mRNA-linker conjugates (Figure 2−4B), which is more than 10 times higher than in our previous study [52,54]. Additionally, we recently also succeeded in releasing cDNA display molecules from SA-beads by using Endonuclease V instead of RNase T1 by designing a new puromycin-linker [55]. Thus, we believe that this new linker and our currently optimized conditions will make cDNA display more useful and practical for *in vitro* proteins/pepties selection.

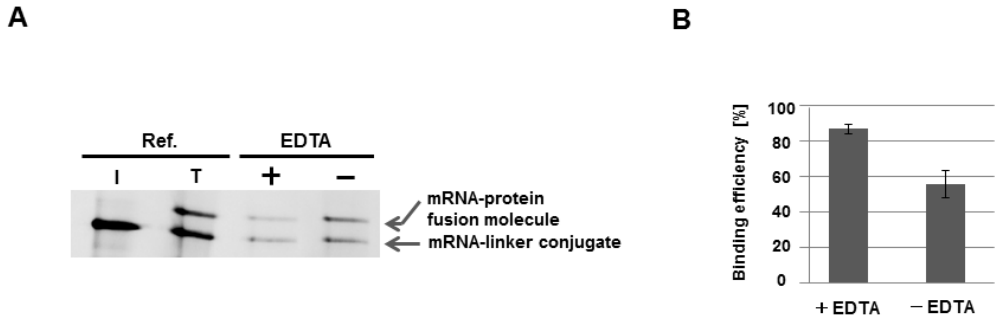

Figure 2–2. Effect of EDTA treatment on the capturing of mRNA-protein fusions by SA-beads. mRNA-protein fusion molecules in the translation reaction mixture with (+) or without (−) EDTA were incubated with SA-beads [the ratio of the biotin-binding capacity of the SA-beads to the total amount of puromycin-linker DNA is 200 to 1]. (A) The remaining mRNA-protein fusion molecules in each translation reaction mixture were analyzed by 4% stacking–6% separating SDS-PAGE containing 8 M urea. The input mRNA-linker conjugates and translation reaction mixture are shown in lane I and lane T, respectively. (B) Binding efficiencies are calculated by: [band intensity of the mRNA-protein fusion molecules in lane T] - [band intensity of the remaining mRNA-protein fusion molecules in each lane indicated by "+" or "–" EDTA].

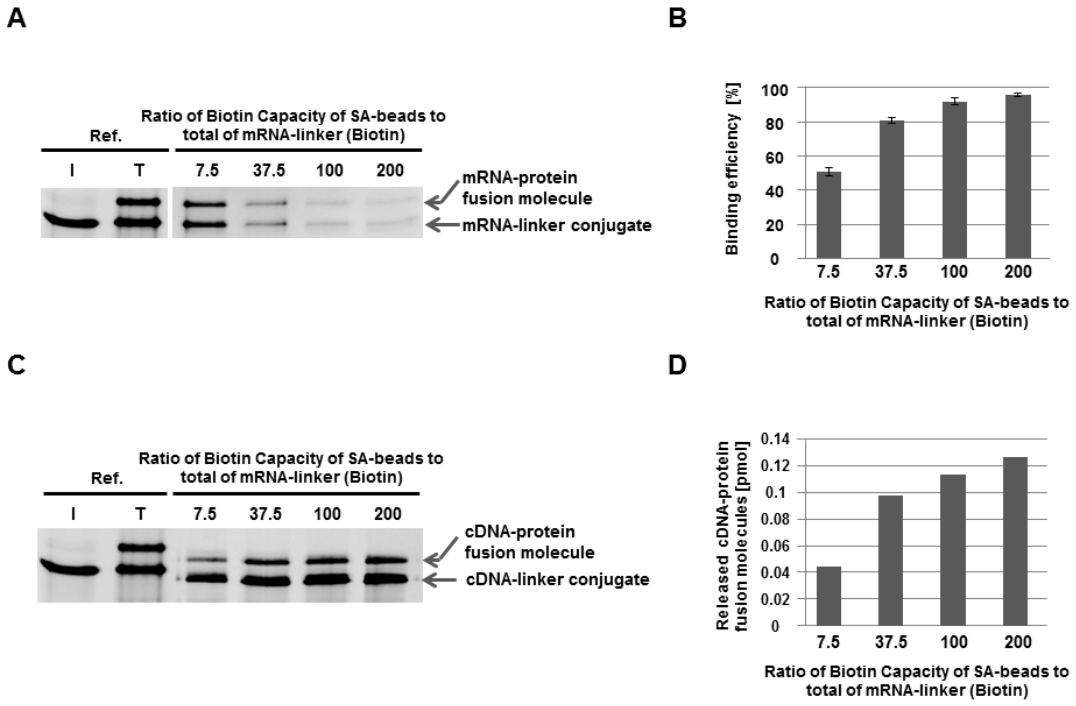

Figure 2–3. Optimization of the amount of SA-beads to bind the mRNA-protein fusion molecules. (A) mRNA-protein fusion was prepared from DNA template coding B domain of protein A (BDA) using SBP-linker as described Figure 2–1. Translation mixture was treated with EDTA same as Figure 2–2. Then mRNA-protein fusion molecules and remained mRNA-linker conjugates were collected with 0.0075–0.2 mg of SA-beads per 0.5 pmol of mRNA estimated from the amount in the ligation reaction [the ratio of the biotin-binding capacity of the SA-beads to the total amount of SBP-linker (containing a single biotin) is 7.5–200]. Inputted mRNA-linker conjugates (lane I), translation mixture (lane T), and remaining mRNA-protein fusion molecules in the translation mixture after incubation with different amounts of SA-beads were analyzed by 4% stacking–6% separating SDS-PAGE containing 8 M urea. (B) Binding efficiencies of each ratio were calculated by: [band intensity of the mRNA-protein fusion molecules in lane T] - [band intensity of the remaining mRNA-protein fusion molecules in each lane indicated by SA-beads]. Experiments were repeated three times. Error bars = standard deviation. (C) mRNA/cDNA-protein fusion molecules were prepared with each ratio of SA-beads. (D) The amount of cDNA-protein fusion molecules calculated by comparing the band intensity between the cDNA-protein fusion molecule of each lane and 0.5 pmol of mRNA-linker conjugate.

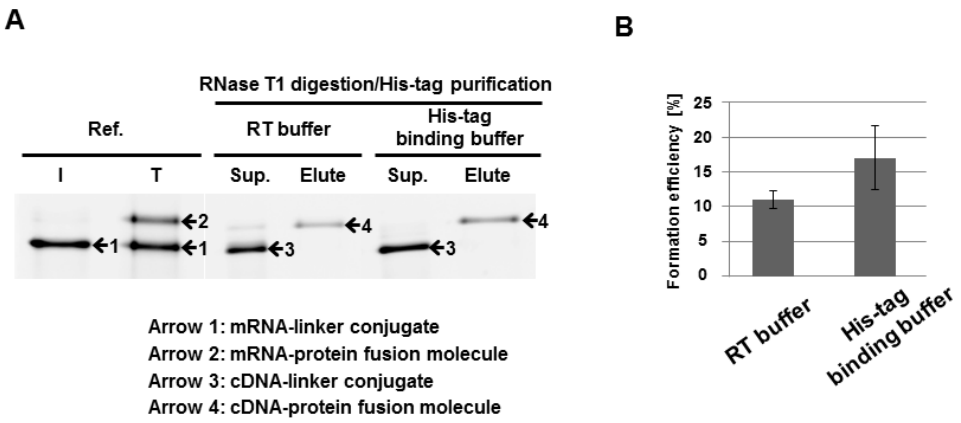

Figure 2–4. Effect of His-tag-binding buffer in RNase T1 digestion and His-tag purification to recover mRNA/cDNA-protein fusion molecules from SA-beads. (A) cDNA-protein fusion molecules were synthesized and released from the SA-beads by RNase T1 treatment in RT reaction mixture or His-tag-binding buffer (20 mM Sodium phosphate, pH 7.4, 500 mM NaCl, 5 mM imidazole, 0.05% Tween-20). cDNA-protein fusions in the each sample were purified with 20 μL of Ni-NTA beads (His Mag Sepharose Ni, GE Healthcare, USA) according to the attached instruction. Inputted mRNA-linker conjugates (lane I), translation mixture (lane T), each supernatant (Sup.) of Ni-NTA beads and eluate were analyzed by 4% stacking–6% separating SDS-PAGE containing 8 M urea. (B) Formation efficiencies of mRNA/cDNA-protein fusion molecules from mRNA-linker conjugates were estimated by comparing the band intensities between the purified cDNA-protein fusion molecule of each lane and that of the mRNA-linker conjugate (lane I). Results are the mean of three independent experiments performed in duplicate. Error bars = standard deviation.

2-2. A pull-down method with a biotinylated bait protein prepared by cell-free translation using a puromycin-linker

2-2-1. Introduction

In directed evolution studies, many candidate molecules, such as peptide aptamers and single-chain variable fragments, have been selected by *in vitro* selection using a cell-free translation system, including ribosome display, mRNA display, and cDNA display as described above. Both cases require that evaluation of many candidate molecules for their affinity against a target molecule be rapid, easy, and low cost via high-throughput techniques. In particular, for *in vitro* selection of disulfide-rich peptide aptamers, kind, rapid, and low cost techniques to confirm affinity of selected sequences against target molecule may be required. Because disulfide connectivity of selected disulfide-rich peptides is unknown at that point, it must be need to analysis disulfide connectivity by some way. In any case, to analysis disulfide connectivity will be a hard work [60]. For the reason, we established a novel pull-down method using a biotinylated bait protein prepared with a puromycin-linker DNA and a cell-free translation system.

2-2-2. Materials and methods

A schematic of the pull-down method and puromycin-linker DNA construct is shown in Figure 2–5. The pull-down method was validated by testing three well known binding partner types: (1) BDA and immunoglobulin G (IgG), (2) FLAG tag and anti-FLAG tag monoclonal antibody (mAb), and (3) mouse Fas ligand (FasL) and anti-FasL mAb. Each BDA, FLAG tag, or FasL was used as a bait protein immobilized on a magnetic bead. The DNA was transcribed into mRNA using the T7 RiboMAX express large scale RNA production system and the synthesized mRNA purified with an RNA purification kit (Qiagen, Germany). A puromycin-linker DNA was hybridized to a purified mRNA, and the 5'-terminus of the puromycin-linker DNA and the 3'-terminus of the mRNA were ligated with T4 RNA ligase and T4 PNK by incubation at 25 ℃ for 60 min. 6 pmol of the ligation product was placed into 50 μL of *in vitro* translation reaction solution with the Retic Lysate IVT kit and incubated at 30 ℃ for 20 min. Then, 20 μL of 3 M KCl and 6 μL of 1 M $MgCl_2$ were added to the sample and incubated at 37 ℃ for 60 min. Further EDTA solution (0.5 M, pH 8.0) was added to the translation reaction and incubated at 25 ℃ for 10 min. RNase One (Promega, USA) was then added to the sample and incubated at 37 ℃ for 20 min to digest the mRNA. Each biotinylated bait protein was captured with 10 μL of Dynabead MyOne Streptavidin C1, and washed three times with 200 μL of 1X binding buffer. 30 μL of each fluorescein-labeled prey protein solution (200 or 400 nM) was incubated at 25 ℃ for 30 min with the magnetic beads on which each

bait-protein immobilized. IgG and anti-FLAG tag mAb (mouse) were purchased from Sigma–Aldrich (USA) and anti-FasL mAb (hamster) from Medical & Biological Laboratories (Japan). Each prey protein was labeled with N-hydroxysuccinimide fluorescein (Pierce, USA) at a ratio of <1.0 dye/protein. After three washing of the beads with 200 μL of phosphate-buffered saline containing 0.1% Tween-20 (PBS-T), the remained prey proteins were eluted by addition of 20 μL SDS sample buffer and incubation at 90 °C for 5 min. The eluates were subjected to 4% stacking–12% separating SDS-PAGE and visualized by a Fluorimager (PharosFX; Bio-Rad, USA). The band intensity in each lane was measured using Quantity One 1-D Analysis Software (Bio-Rad, USA).

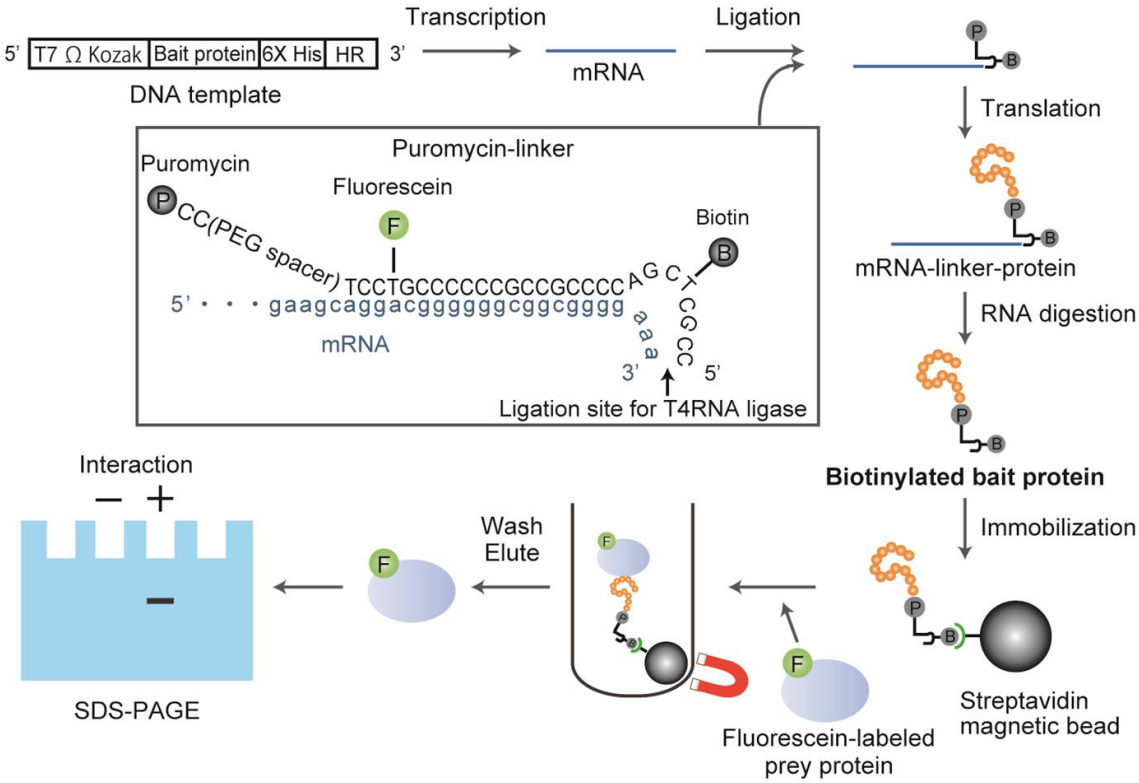

Figure 2–5. Scheme of the pull-down method using a novel puromycin-linker with a cell-free translation system. Bait-protein-coding DNA template is transcribed into mRNA by T7 polymerase. A puromycin-linker NDA is hybridized to the mRNA, and the 5'-terminus of the puromycin-linker DNA and 3'-terminus of the mRNA are ligated with T4 RNA ligase and T4 PNK. The ligation product is *in vitro* translated. Then, mRNA is digested with RNase One. Biotinylated bait protein is captured with SA-beads and prey protein solution (200 or 400 nM) is incubated with the each magnetic bead. The binding prey proteins are eluted and are analyzed by SDS-PAGE and visualized by the Fluorimager.

2-2-3. Results and discussion

The relative SDS-PAGE band intensities of the four types of prey protein against each bait protein are shown in Figure 2–6 and, as expected, the interactions of known binding pairs were detected (Figure 2–6). The relative intensity of pulled-down proteins roughly depended on the dissociation constant for each interaction (i.e., IgG ≅ anti-FLAG tag mAb < anti-FasL mAb). The affinity of each protein pair interaction was in the submicromolar to nanomolar range [61-63]. In the case of FasL and anti-FasL mAb, anti-FasL mAb was most pulled down by FasL. However, it appeared that anti-FasL mAb was also pulled down slightly by BDA in comparison with negative controls. This may have occurred naturally because BDA affinity towards antibodies depended on the antibody species subclass. In general, it is known that BDA binds more strongly to a hamster antibody (anti-Fas mAb) than a mouse antibody (anti-FLAG mAb) [64]. From the differences in band intensities between anti-FasL mAb and other negative controls, we concluded that this pull-down method could be applied to protein–molecular interaction analysis in the micromolar range of dissociation constants. Furthermore, whether the amount of pulled-down bait protein depended on the prey protein concentration was examined by testing the pull-down of the anti-FLAG tag mAb as a prey protein at two different concentrations (400 and 200 nM). Although anti-FLAG tag mAb was pulled down at both concentrations under the same conditions, anti-FLAG tag mAb at 400 nM was pulled down more than at 200 nM. This meant that the optimization of prey

protein concentration against a bait protein will be required if the band intensity of the prey protein is weak. Fluorescent labeling of the prey protein is valuable for rapid and convenient analysis by SDS-PAGE. On the other hand, Western blotting could also be useful for detection of pulled-down protein, which may be particularly important if the molecular probes used for fluorescence could interfere with protein–protein interactions. In general, pull-down assays are useful as an initial screening assay to identify previously unknown protein–protein interactions as well as to confirm the existence of a protein–protein interaction predicted by other research techniques, such as coimmunoprecipitation [65,66]. In this case, a bait protein is tagged and captured on an immobilized affinity ligand specific for the tag (e.g., glutathione S-transferase-tagged or His-tagged). Thus, the use of a protein that is easily biotinylated *in vitro* as an alternative to other tagged proteins as the pull-down driver is a promising tool because of the high-affinity interaction between biotin and streptavidin [67]. However, protein biotinylation by methods, such as amine-reactive biotinylation, may critically interfere with a protein's molecular interactions. Using the present method, biotin was conjugated at the prey protein C-terminus via a polyethylene glycol spacer with a puromycin-linker DNA, such that the prey protein immobilized on a streptavidin bead interacted with the bait protein without interference from biotin adducts on the protein surface. Usually, bait proteins are prepared by Escherichia coli expression or chemical synthesis, which is time-consuming, laborious, and expensive. One of the advantages of the present method was that the requisite amount of bait

proteins for an assay could be prepared easily and rapidly at low cost by combination of the puromycin-linker with a cell-free translation system. Furthermore, the synthesized bait protein could be easily analyzed by SDS-PAGE and the Fluorimager, because the puromycin-linker has a fluorescein as well as a biotin moiety (Figure 2–5). In general, it was very difficult to detect a synthesized bait protein in a crude sample because the amount of protein synthesized in a cell-free translation system was very low. Ultimately, for the above reasons, many candidate bait proteins could be assayed simultaneously within 1–2 days using this pull-down method. In conclusion, a puromycin technique-based pull-down method was developed for evaluating protein–protein interactions semi-quantitatively in a multisample-processing manner by rapid and simple biotin modification of a bait protein using a cell-free translation system. It is expected that this method will be suitable for high-throughput assays of protein–protein interactions, which are required by genome-wide proteomics and *in vitro* affinity selection of proteins and peptides.

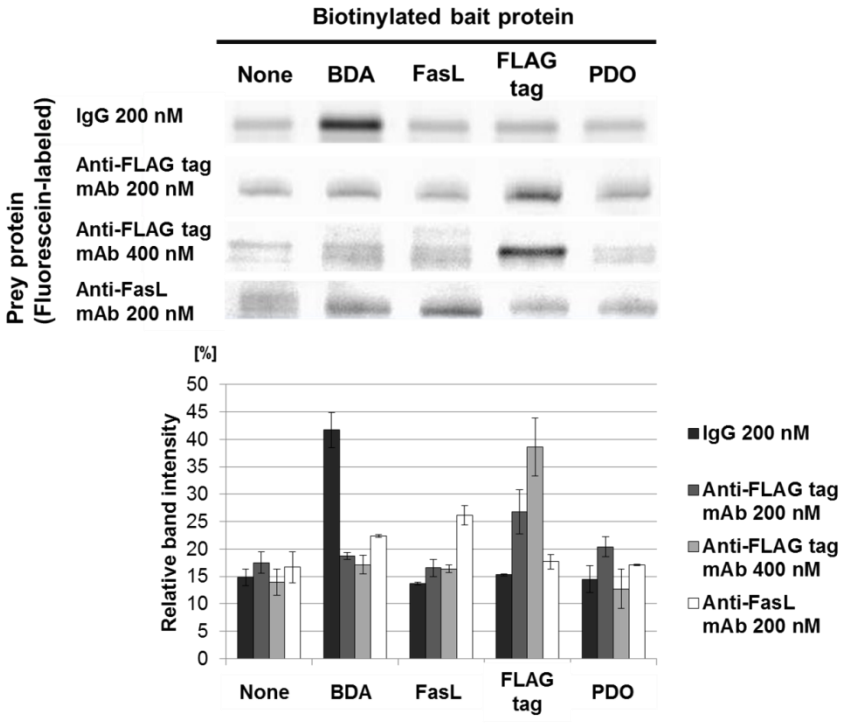

Figure 2–6. Evaluation of protein–protein interactions by the pull-down method. Four types of magnetic bead with immobilized bait proteins (BDA, FasL, FLAG tag, and Pou-specific DNA binding domain of Oct1 (PDO, a bate protein as negative control)) and magnetic beads immobilized puromycin-linker only (None; negative control) were prepared and incubated with each prey protein (IgG, anti-FLAG tag mAb, and anti-FasL mAb). Pulled-down prey proteins were analyzed by 4% stacking–12% separating SDS-PAGE and visualized by the Fluorimager. The band intensity of each lane was measured using analysis software and relative band intensities of the four types of prey protein against each bait protein are shown here (bottom). Values are means ±standard error (n = 3).

2-3 Conclusions

We improved the yield of cDNA display molecules from mRNA molecules more than 17 times higher than in our previous study [52,54] by the optimization of preparation procedure. This is actual increasing of the library size. On the other hand, we established a pull-down method using a puromycin-linker and a cell-free translation, which may be used to confirm selected peptide functions. These enable *in vitro* selection of peptide aptamers by cDNA display method more user friendly and effective method to design desired peptides.

Chapter 3: *In vitro* selection of disulfide-rich peptides against amino groups by cDNA display method

3-1. Introduction

In vitro selection of peptides from a wide variety of libraries is a powerful approach for the development of peptide aptamers against several target molecules/materials. Indeed, various peptide aptamers have been successfully designed to select against not only proteins but also several types of materials, including metals, metal oxides, metal compounds, polymeric materials, semiconductors and carbon materials [18-20]. The material-binding peptides can be used as functional nanomaterials such as surface modifying absorbents for patterning and as catalysis for the preparation of inorganic particles. The material-binding peptides are comparably short in length, ranging between 7 and 21 residues in length, and some peptides have a cyclic form with a disulfide bridge [14]. In many cases, the cyclization of a peptide can improve affinity and specificity, whereas in some cases, cyclization has no or even a negative influence on material binding [68]. As described here, peptides have been useful reagents for molecular recognition.

Nonetheless, there are only a few examples in the literature of *in vitro* selection of small molecule-binding peptides [69-73]; thus small molecule recognition by peptides remains an unexplored territory. Peptides generally cannot adopt structures that have a cavity or pocket for small

molecule recognition and binding, and there has been no effective strategy to design peptides that can bind small molecules. In order to develop a peptide as a useful affinity reagent that is an alternative to antibodies, more studies describing improvements in the molecular recognition ability of peptides are required.

In medicine, constrained peptides, such as disulfide-rich peptides including venom peptide ‘conotoxins’ and polycyclic peptides [74], have been investigated because of their extreme specificity and affinity towards a target protein. However, molecular recognition ability of constrained peptides containing disulfide bonds against non-protein target molecules including small molecules has not been investigated. Thus, we examined how a constrained peptide containing disulfide bridges can enhance the molecular recognition ability towards non-protein molecules.

In the cDNA display method, the disulfide bridges in the displayed peptide easily form on magnetic beads during the preparation process [52,54]. Thus, this method is suitable to screen target molecule-binding disulfide-rich peptides from a DNA library of coding cysteine-rich peptides in which the cysteine position is randomized. In this study, an amino group on the polystyrene-based magnetic bead was chosen as the low molecular weight target, because a functional group recognizing peptides has not been reported.

3-2. Materials and methods

3-2-1. Library construction

A full construct for preparing the disulfide-rich peptide library was designed to facilitate the formation and purification of cDNA displayed proteins. The full-sequence of the library contains the T7 promoter, a translational enhancer derived from tobacco mosaic virus ‘omega’, and a Kozak sequence at the 5' site of the disulfide-rich peptide coding region, whereas the G_3S spacer, C-terminal 6×His, G_2S spacer and primer region for the SBP-linker were placed at the 3' site (Figure 3–1A). The amino acid composition of the library was adjusted by the nucleotide mixture (Figure 3–1B, Table 3–1). The library DNA was prepared by joining the three fragments by overlap PCR. Each DNA fragment is as follow: (i) fragment 1, sense ssDNA composed of the T7 promoter to an ATG start codon; (ii) fragment 2, antisense ssDNA corresponding to the disulfide-rich peptide coding region; and (iii) fragment 3, antisense ssDNA that consists of the His×6 coding region and the hybridizing region for the SBP-linker (Table 3–1). Initially, fragments 1 and 2 were overlapped and extended with Taq DNA polymerase (Takara Bio, Japan). This was followed by fragment 3 overlapping to the synthesized double strand (ds) DNA and extended. The resulting full-construct DNA was purified by 8 M urea containing 6% denaturing PAGE. Purified full-construct ssDNA was converted to dsDNA by five cycles of PCR for transcription.

(A)

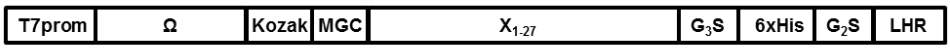

(B)

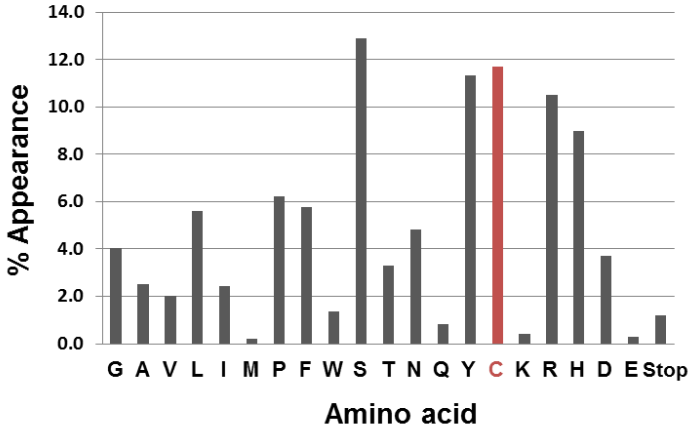

Figure 3-1. The library DNA construct and amino acid composition of the random region. (A) Construct of library DNA coding cysteine-rich peptides. Symbols and abbreviations are defined as follows: T7prom, T7 promoter; Ω, translation enhancer of tobacco mosaic virus; Kozak, Kozak sequence for translation initiation; MGC, N-terminal three constant amino acids; $X_{1\text{-}27}$, twenty seven randomized amino acids; G_3S and G_2S, glycine-serine linker; 6×His, hexahistidine tag; and LHR, hybridization region for puromycin-linker DNA. (B) Theoretical percent appearance of amino acids in the random region.

Table 3–1. DNA fragments for synthesis of cysteine-rich peptide coding library DNA.

Name	Sequence (5'→3')
Fragment 1 (sense strand)	GATCCCGCGAAATTAATACGACTCACTATAGGGGAAGTATTTTTACA ACAATTACCAACAACAACAACAAACAACAACAACATTACATTTTAC ATTCTACAACTACAAGCCACCATG
Fragment 2 (antisense strand)	TGATGATGGCTGCCTCCCCCXYZXYZXYZXYZXYZXYZXYZXYZXY ZXYZXYZXYZXYZXYZXYZXYZXYZXYZXYZXYZXYZXYZXYZXY ZXYZXYZXYZGCAGCCCATGGTGGCTTGT
Fragment 3 (antisense strand)	GGGGGAGGCAGCCATCATCATCATCACGGCGGAAGCAGGACG GGGGGCGGCGGGGAAA

Random amino acid comprised the codon triplets XYZ, where X, Y, and Z indicate nucleotide mixture, and the mixing ratios were X: A 44%, T 0%, G 38%, C 22%; Y: A 16%, T 30%, G 20%, C 34%; Z: A 45%, T 15%, G 30%, C 10% or X: A 50%, T 0%, G 50%, C 0%; Y: A 16%, T 33%, G 20%, C 31%; Z: A 35%, T 18%, G 32%, C 15%.

3-2-2. SBP-linker synthesis

SBP-linker was prepared from two modified oligonucletoides (Table 3–2) Immediately prior to use, The 5' thiol group of 20 nmol of puromycin segment was reduced with 0.1 M DTT in 50 μL of 1 M phosphate buffer (pH 7.0) for 1 h at room temperature and then desalted on a NAP-5 column (GE Healthcare, USA). A total of 10 nmol of short biton segment and 2 μmol EMCS were added to 100 μL of 0.2 M sodium phosphate buffer (pH 7.0), and the mixture was incubated for 30 min at 37 °C, then precipitated with ethanol and coprecipitant (Quick-precip Plus, Edge BioSystems, USA), and dissolved in nuclease-free water. The reduced PS was immediately added and the mixture was stirred at 4 °C overnight. The reaction was terminated by adding DTT to a final concentration of

50 mM and incubating for 30 min at room temperature. Ethanol precipitation at room temperature was performed to remove the excess PS. To remove the SBS and the un-cross-linked SBS-EMCS complexes, the ethanol precipitate was dissolved in nuclease-free water and purified with a C18 HPLC column using the following conditions: column, AR-300, 4.6×250 mm (Nacalai Tesque, Japan); solvent A, 0.1 M triethylammonium acetate (TEAA); solvent B, acetonitrile/water (80:20, v/v); gradient, B/A (15–35% over 33 min); flow, 0.5 mL/min; detected by absorbance at 260, 280, and 490 nm. The fraction corresponding to the last peak at an absorbance of 260 (corresponding to a single peak at an absorbance of 490 nm) was collected. The fraction was dried and the SBP-linker was purified by ethanol precipitation using Quick-precip Plus. Precipitated SBP-linker was dissolved in nuclease-free water and stored at -20 °C.

Table 3–2. DNA fragments for synthesis of SBP-linker

Name	Sequence (5'→3')	Length	modification
Short biotin segment	CCgCBCgACCCCGCCGCCCCCCGtCCT	27 mer	g: riboG, B: Biotin-dT, t: AminoC6-dT
Puromycin segment	(5S)TCFZCCP	8 mer	5S: 5'-ThiolC6, F: FITC-dT, Z: Spc18, P: 3'-Puromycin

3-2-3. cDNA display preparation from library DNAs

The library DNAs were transcribed by T7 RNA polymerase in a RiboMAX large scale RNA production system. Reactions were terminated by adding DNase and products were purified with an RNA purification column (FavorPrep, After Tri-Reagent RNA Clean-Up Kit, Favorgen, Taiwan).

The 3'-ends of mRNA molecules were hybridized to the complementary strands of the SBP-linker under annealing conditions (heating to 90 ℃ for 1 min followed by incubation at 70 ℃ for 1 min, then cooling to 25 ℃) in ligation buffer (50 mM Tris-HCl, pH 7.5, 10 mM $MgCl_2$, 10 mM DTT and 1 mM ATP). T4 RNA ligase (0.4–2 U/pmol mRNA, Takara Bio, Japan) and T4 PNK (0.25 U/pmol mRNA) were then added and the reaction incubated at 25 ℃ for 1 h. The ligation products were analyzed using 8 M urea containing 6% PAGE. The ligated products (mRNA-linker conjugates) were visualized by FITC fluorescence using the Fluoroimager.

2X Binding buffer (20 mM Tris-HCl, pH 7.5, 2 M NaCl, 2 mM EDTA, 0.1% Tween-20) was added to the ligation reaction mixture and incubated with SA-beads (Dynabeads MyOne Streptavidin C1) at a ratio of 3.75 μL of SA-beads to 1 pmol of mRNA-linker conjugates at 20 ℃ for 15 min. After washing with 1X binding buffer, the SA-beads were incubated at 30 ℃ for 25 min in a cell-free translation mixture with a rabbit reticulocyte lysate (Retic Lysate IVT Kit) at the ratio of 10 μL of SA-beads to 20 μL of the cell-free translation mixture. To facilitate puromycin

incorporation to the C-terminus of the peptide, KCl and $MgCl_2$ were added to the mixture (final conc. of 800 and 80 mM, respectively) and incubated at 37 ℃ for 60 min. Then, to release ribosomes binding to the mRNA, a pure 0.5 M EDTA solution was added (final conc. of 83 mM) and incubated at r.t. for 10 min.

The SA-beads were washed three times with 1X binding buffer and once with 1X buffer for the reverse transcription reaction that is attached to a reverse transcription enzyme (ReverTra Ace, Toyobo, Japan). The reverse transcription reaction mixture (1 mM dNTP, 2.5 U/μL ReverTra Ace in 1X buffer) was mixed with the SA-beads at the ratio of 15 μL of SA-beads to 10 μL of the mixture, and incubated at 42 ℃ for 30–45 min. After washing the SA-beads with the His-tag-binding buffer (20 mM sodium phosphate, pH 7.4, 0.5 M NaCl, 5 mM imidazole, 0.05% Tween-20), the His-tag-binding buffer with 5 U/μL RNase T1 (Ambion, USA) was mixed with the SA-beads at the ratio of 30 μL of SA-beads to 10 μL of the buffer containing RNase T1, and incubated at 37 ℃ for 15 min. The supernatant containing the cDNA display molecules was collected.

To purify cDNA display molecules using the His×6 tag in displayed peptides, the solution containing the cDNA display molecules was incubated with Ni-NTA magnetic beads (His Mag Sepharose Ni, GE Healthcare, USA) at 10 ℃ for over 2 h. The Ni-NTA magnetic beads were washed twice with His-tag-binding buffer, and binding cDNA display molecules were eluted by

incubation at r.t. for 10 min in the His-tag elution buffer (20 mM sodium phosphate, pH 7.4, 0.5 M NaCl, 250 mM imidazole, 0.05% Tween-20). The above elution step was performed twice under the same conditions. Before affinity selection of the disulfide-rich peptides from the cDNA display library was carried out, the His-tag elution buffer was exchanged to the selection buffer (50 mM Tris-HCl, pH 7.4, 1 M NaCl, 1 mM EDTA, 0.1% Tween-20) with 1 μM L-cystine using Micro Bio-Spin columns with Bio-Gel P-6 in Tris Buffer (BioRad, USA). cDNA display molecules prepared from 10 pmol of library mRNA were digested with 10–30 U of RNase H (Takara Bio, Japan) in NEBuffer 2 (10 mM Tris-HCl, pH 7.9, 50 mM NaCl, 10 mM $MgCl_2$, 1 mM DTT) by incubating at 37 °C for 20 min. The resulting cDNA-protein fusion molecules were subjected to 8 M urea containing 4% stacking–6% SDS-PAGE and visualized with the Fluoroimager.

3-2-4. Affinity selection

The above disulfide-rich peptide library was screened to identify peptides that selectively bound to the amino group, using Dynabeads M-270 Amine (Invitrogen, USA). The initial round contained cDNA display molecules prepared from 150 pmol of library mRNA in 70 μL of selection buffer. This was incubated at r.t. for 1.5 h using a tube rotator (AS ONE, Japan) with 50 μL of Dynabeads M-270 Amine, which was prewashed using the selection buffer with 100 nM L-cystine. The beads were washed four times using the selection buffer with 100 nM L-cystine. To elute amino

group binding cDNA display molecules, the beads were incubated at r.t. for 1 h in 400 μL of selection buffer containing 0.1 M DTT. This was followed by incubation at 4 °C for 4 h. This was then incubated at r.t. for 1 h using a micro tube mixer (Tomy Seiko, Japan) in 400 μL of selection buffer with 1% SDS. cDNA display molecules in each eluate were ethanol precipitated using ethanol-precipitation Quick-precip Plus. To prepare library DNAs for the next round of *in vitro* selection, T7 promoter-reconstructed library DNAs were prepared from the above precipitated cDNA display molecules by PCR using the following primers: forward primer (5'-GATCCCGCGAAATTAATACGACTCACTATAGGGGAAGTATTTTTACAACAATTACCAACAAC-3'); reverse primer (5'-TTTCCCCGCCGCCCCCCGTCCTGCTTCCGCCGTGATGAT-3').

A total of four rounds of *in vitro* selection were performed according to the above protocol with minor changes as follows. The cDNA display library was prepared from 30 pmol mRNA in the second round and 20 pmol in the third and fourth rounds. The target bead volume was successive reduced from 50 to 30 μL, and cDNA molecules that can bind to the bead material were removed by prescreening using Dynabeads M-270 Carboxylic Acid (Invitrogen, USA).

After the fourth round of *in vitro* selection, alternation of sequence composition in the library DNAs was confirmed by direct sequencing. The library DNAs were then cloned by the pGEM-T Easy Vector System (Promega, USA) and NEB 5-alpha competent *E. coli* (high efficiency) (New England Biolabs, UK), and a total of 90 clones were sequenced by Operon Biotechnologies

(Japan).

3-2-5. Peptides

The peptides analysed in this study are listed in Table 3–3. A FAM-G_3S linker was introduced to the N-terminal of all synthesized peptides for ease of detection except for CP1 (2SS) in which FAM was not attached. Three disulfide isomers of CP1 (2SS): CP1 (2SS)-α, β, and γ; and two kinds of fragmented peptides, the N-terminal or C-terminal loop regions of CP1 (2SS)-α: CP1 (1SS)-NTR and CP1 (1SS)-CTR were chemically synthesized by Toray Research Center, Japan. CP1 (2SS); two kinds of serine variants of CP1 (2SS)-α: CP1 (1SS)-A and B; and an alanine variant of CP1 (2SS)-α: CP1 (Cys→Ala) were chemically synthesized by SCRUM (Japan). All peptides were certified at more than 90% purity.

Table 3–3. Synthesized peptide list.

No.	Name	Size (aa)	Disulfide bridge	Amino acid sequence (N→C)
1	CP1(2SS)[1]	34	Unknown	GGGSMGCGPSNFDDCPRNYTFNSIDSGYCSGCNH
2	CP1(2SS)-α	34	C7-C15 and C29-C32	FAM-GGGSMGCGPSNFDDCPRNYTFNSIDSGYCSGCNH
3	CP1(2SS)-β	34	C7-C29 and C15-C32	FAM-GGGSMGCGPSNFDDCPRNYTFNSIDSGYCSGCNH
4	CP1(2SS)-γ	34	C7-C32 and C15-C29	FAM-GGGSMGCGPSNFDDCPRNYTFNSIDSGYCSGCNH
5	CP1(Cys→Ala)	34	–	FAM-GGGSMGAGPSNFDDAPRNYTFNSIDSGYASGANH
6	CP1(1SS)-A	34	C7-C15	FAM-GGGSMGCGPSNFDDCPRNYTFNSIDSGYSSGSNH
7	CP1(1SS)-B	34	C29-C32	FAM-GGGSMGSGPSNFDDSPRNYTFNSIDSGYCSGCNH
8	CP1(1SS)-NTR	15	C7-C15	FAM-GGGSMGCGPSNFDDC
9	CP1(1SS)-CTR	15	C5-C8	FAM-GGGSCSGCNH

[1]Disulfide bonds were formed by air oxidation.

3-2-6. Trypsin digestion and mass spectrometry analysis

Ten micrograms of CP1 (2SS) was incubated at 37 ℃ for 30 min in 52 μL of trypsin solution (100 mM Tris-HCl, pH 8.0, 1 mM $CaCl_2$, 2 μg trypsin (Trypsin Protease, MS Grade, Thermo Fisher Scientific, USA)). One microliter of the solution and 4 μL of a saturated solution of α-cyano-4-hydroxy-cinnamic acid in TA solution (mixture of 0.1% trifluoroacetic acid and acetonitrile in the ratio of 2:1) were mixed. One microliter of the mixed solution was spotted onto a target plate and dried in a desiccator, and analyzed with a matrix-assisted laser desorption-ionization time-of-flight mass spectrometer (MALDI-TOF MS, Autoflex III, Bruker Daltonics, USA).

3-2-7. Binding assay against amino group modified magnetic beads

Ten microliters of Dynabeads M-270 Amine and of Dynabeads M-270 Carboxylic acid were washed with 100 μL of selection buffer. Three kinds of disulfide isomers of CP1 (2SS) were dissolved in PBS (1mg/mL) and diluted to 2 μM with selection buffer. Thirty microliters of the each 2 μM peptide solution was incubated with the each kind of magnetic beads at 25 ℃ for 2 h using a thermo block rotator (SNP-24B, Nissinrika, Japan). The beads were washed twice with 100 μL of selection buffer and binding peptides were eluted by incubation at 85 °C for 3 min in 20 μL of SDS sample buffer (125 mM Tris-HCl, pH 6.8, 8 M urea, 4% (w/v) SDS, 6% (w/v) sucrose, optimal a

suitable amount of xylene cyanol). Eluate was subjected to Tricine-SDS-PAGE and visualized with the Fluoroimager.

3-2-8. Binding assay against a glass slide

Twenty microliters of solutions containing each disulfide isomer or alanine variant of CP1 (2SS) in selection buffer (without Tween-20) (final conc. of 20 μM) were spotted on a glass slide (MAS coated glass slide, Matsunami Glass, Japan) and incubated at r.t. for 2 h. Remained solutions was removed and the each spotted regions were washed four times with 20 μL of selection buffer by pipetting. The glass slide was dipped in selection buffer for 1 h. Then the glass slide was removed from the buffer and peptides remaining on the glass slide were visualized with the Fluoroimager.

3-2-9. Binding assay against agarose beads

One hundred microliters of diaminodipropylamine-immobilized agarose beads (Calboxylink Coupling Gel, Thermo, USA, 50% slurry) was poured in a 1.5 mL microcentrifuge tube and washed three times with 900 μL of selection buffer by centrifugation of the beads and removing the supernatant. After removing the supernatant as possible by pipetting (about 50 μL volumes of swollen agarose beads was remained in the tube), 30 μL of each 172 μM peptide solution were added to the tube, then mixed and incubated at 25 °C for 2 h. After washing the agarose beads twice with

300 µl of selection buffer, 40 µL of 2X SDS sample buffer was added to elute the binding peptides. The SDS sample buffer was separated from the agarose beads with an empty column (MicroSpin Empty Columns, GE Healthcare, USA). 70 µL of eluate was collected and 2 µL of it was analyzed by Tricine-SDS-PAGE.

3-2-10. Circular dichroism analysis

Circular dichroism (CD) spectra were recorded at 25 ℃ in 0.1 mm cell from 250 to 195 nm at 50 nm/min on a circular dichroism spectrometer (J-720, JASCO, Japan). Peptides were dissolved (0.2 mg/ml) in 20 mM sodium phosphate buffer, pH 7.4. Spectra were measured four times and averaged for each sample, and an equally averaged buffer baseline was subtracted.

3-3. Results and discussion

3-3-1. *In vitro* selection of amino group binding peptides

After four rounds of the selection, the library DNA was sequenced by direct sequencing (Figure 3–2). The signal pattern of the random peptides coding region of the DNA library following the fourth round was different with that of the initial library. This suggested that the specific peptide sequences were enriched by *in vitro* selection. Then, DNA molecules in the library after the fourth round were cloned and 90 clones were sequenced. As a result, the library seems to be converged to several sequences as shown in Table 3–4. The CP1 peptide is the most converged sequence, whereas the other peptides in the CP1 group have single or double amino acid substitutions.

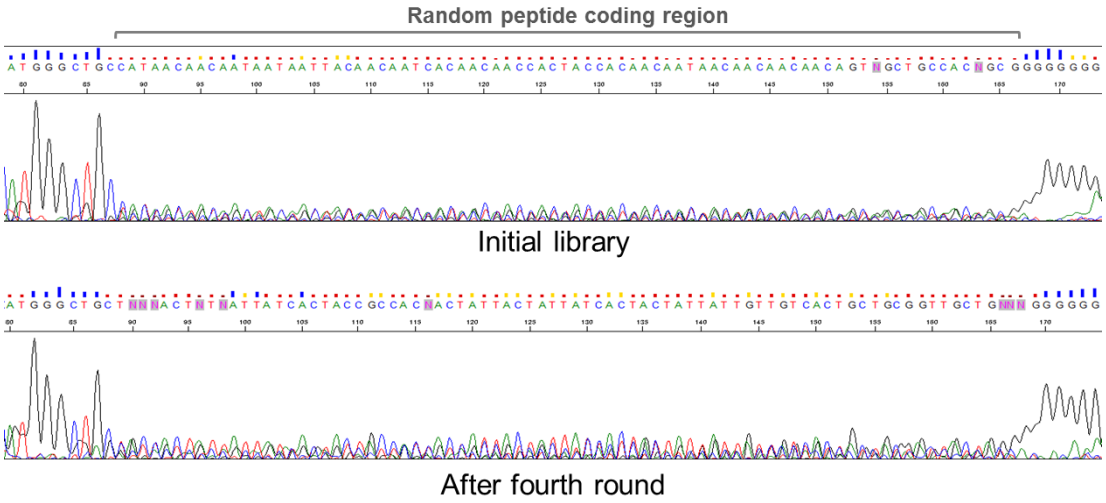

Figure 3–2. Direct sequencing of the initial and following the fourth round library DNA. Initial library (upper) DNA and library DNA after the fourth round of *in vitro* selection (lower) were sequenced by direct sequencing of the PCR products. Predominantly random peptide coding regions in each library DNA are indicated.

Table 3–4. List of the consensus peptide sequences from the library after the fourth round.

Name	Sequence	No. of clones
Library	MGCXXXXXXXXXXXXXXXXXXXXXXXXX	
CP1	MGCGPSNFDDCPRNYTFNSIDSGYCSGCNH	**10**
CP1-2	MGCGPSNFDDCPRDYTFNSIDSGYCSGCNH	**1**
CP1-3	MGCGPSNFDDCPRNYTFNPIDSGYCSGCNH	**1**
CP1-4	MGRGPSNFDDCPRNYTFNSIDSGYCSGCNH	**1**
CP1-5	MGCGPSNFDDCPRDYTFNPIDSGYCSGCNH	**1**
CP1-6	MGCGPSNFDDCPRNYTFNPIDSGHCSGCNH	**1**
CP2	MGCTQFQGVRPSNCKCTCSGFYRYLYPFWA	**1**
CP2-2	MGCTQFQGLRPSNCKCTCPGFYRYLYPFCA	**1**
CP3	MSWPWHRTHHSYNPWYHYWYRYPTRYRHFS	**5**

3-3-2. Binding assay by a pull-down method

Disulfide connectivity of CP1 with function had been unknown, thus CP1 was chemically synthesized and disulfide bridges were formed by air oxidation. Affinity of the CP1 was assayed by pull-down assay in crude condition of disulfide isomers of CP1 (2SS) (Figure 3–3). As a result, CP1 (2SS) was significantly pulled down by each kind of magnetic beads compared with a alanine variant of CP1: CP1 (Cys→Ala). This result shows that the CP1 (2SS) can interact with each kind of magnetic beads.

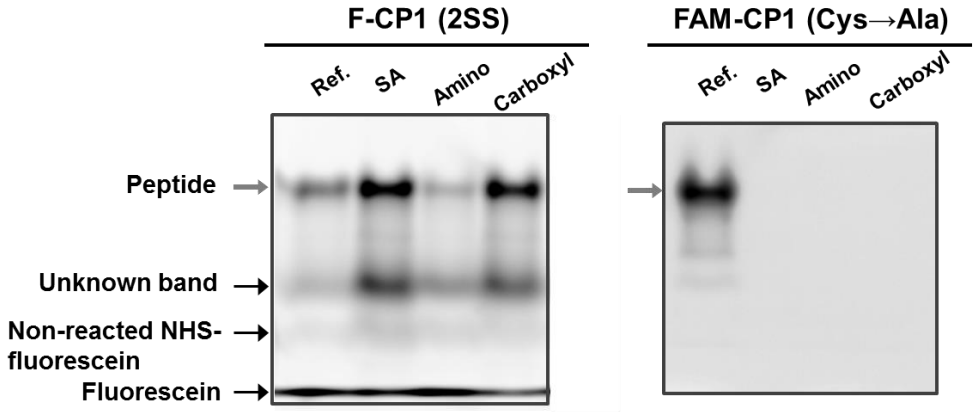

Figure 3–3. Pull-down assay of CP1 (2SS) and CP1 (C→A). N-terminus of CP1 (2SS) was modified by fluorescein-NHS: F-CP1 (2SS). 30 μL of 2 μM F-CP1 (2SS) and CP1 (Cys→Ala) were incubated at r.t. for 1 h with 10 μL of Dynabeads MyOne Strptavidin C1 (SA) or Dynabeads Amine (Amino) or Dynabeads Carboxylic Acid (Carboxyl). These beads were washed three times with 100 μl of Tris-based buffer (20 mM Tris-HCl, pH 6.8, 1 M NaCl, 0.1% Tween-20). Binding peptides on these beads were eluted by incubation at 85 ℃ for 3 min in 20 μL of 1X SDS sample buffer and analyzed by Tricine-SDS-PAGE.

3-3-3. Analysis of the relationship between disulfide connectivity and function

To analyze the relation between the disulfide bond connectivity of CP1 and function, CP1 (2SS) was digested with trypsin and the digested peptide fragments were analyzed by MALDI-TOF MS (Figure 3-4). Trypsin cleaves peptide chains mainly on the carboxyl side of lysine or arginine amino acids, except when either is followed by proline. Following trypsin digestion, the main peak was found to (1654.727 m/z) correspond to an N-terminal fragment of CP1 (C7–C15:C29–C32). Although a second peak (1879.803 m/z) was weak, it may correspond to the C-terminal fragment of CP1 (C7–C15:C29–C32). On the other hand, the peak which was speculated to arise following the trypsin digestion of CP1 (C7–C29:C15–C32) and CP1 (C7–C32:C15–C29) was barely detected.

From the above MS analysis of CP1 (2SS) with trypsin digestion, we speculate that CP1 (C7–C15:C29–C32) was the main peptide in the crude mix of the disulfide isomers of CP1 (2SS) and it may bind to the amino group on the Dynabeads M-270 Amine. To clarify the relation between disulfide connectivity and binding affinity, three kinds of disulfide isomers of CP1 (2SS) were chemically synthesized (Table 3–3). Interaction of the each disulfide isomer of CP1 (2SS) was confirmed by a pull-down assay (Figure 3–5). As a result, CP1 (2SS)-α was found to only bind to the Dynabeads M270 Amine and Carboxylic acid. These results suggest that the disulfide connectivity pattern was important for defining the affinity of the CP1.

The pull-down assay was performed under reducing condition to ascertain the importance of the disulfide bridges in CP1 (2SS)-α capacity to interact with the beads. As a result, CP1 (2SS)-α was not pulled down under reducing conditions with DTT (Figure 3–6). This result shows that the disulfide bridges in CP1 (2SS)-α are crucial to the affinity. This result was consistent with the result that substitution of all cysteines to alanines gave rise to a CP1 (2SS)-α peptide with no binding affinity (Figure 3–3).

The actual disulfide bond connectivity of CP1 (2SS) corresponded to the predicted result derived from Disulfind: Cysteines Disulfide Bonding State and Connectivity Predictor (Disulfind: a disulfide bonding state and cysteine connectivity prediction server) [75]. Furthermore, we compared the mobility of each disulfide isomer of CP1 and CP1 (2SS) by Tricine-SDS-PAGE (Figure 3–7, left). The main band that appeared in the CP1 (oxidized) lane in the case of the oxidized form corresponded to the mobility of CP1 (2SS)-α. As a control, the reduced form of each disulfide isomer of CP1 (2SS) showed the same mobility (Figure 3–7, right). In the case of pretreatment with 2-mercaptoethanol, double bands were observed in each lane. This is a result of partially oxidative folding of CP1 during Tricine-SDS-PAGE, because of the non-reducing conditions used in the Tricine-SDS-PAGE gel. These results show that CP1 may easily adopted CP1 (2SS)-α fold in oxidative folding. These results may indicate that the selected disulfide-rich peptides that exhibited the function had the most dominant disulfide connectivity. In other words, the cDNA display method

can select disulfide-rich peptides that easily formed specific disulfide connectivity and thereby exhibit function. This may be an advantage with regard to production of disulfide-rich peptides selected by *in vitro* selection, because generally, specific disulfide bridge formation in disulfide-rich peptides is difficult and requires purification by HPLC [76].

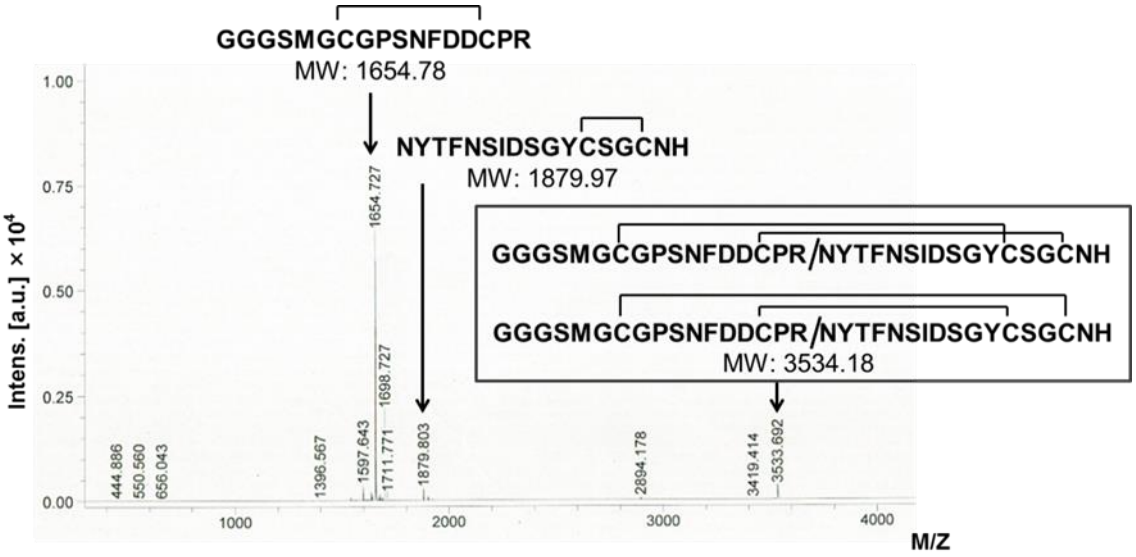

Figure 3–4. MALDI-TOF MS analysis of the trypsin-digested CP1 (2SS). CP1 (2SS) was digested with trypsin by incubation at 37 °C for 30 min and the digested peptide fragments were analyzed by MALDI-TOF MS. Peptide sequences corresponded to several peaks were estimated and shown over each peak. The MW under each peptide sequence indicates the theoretical values of the molecular weight.

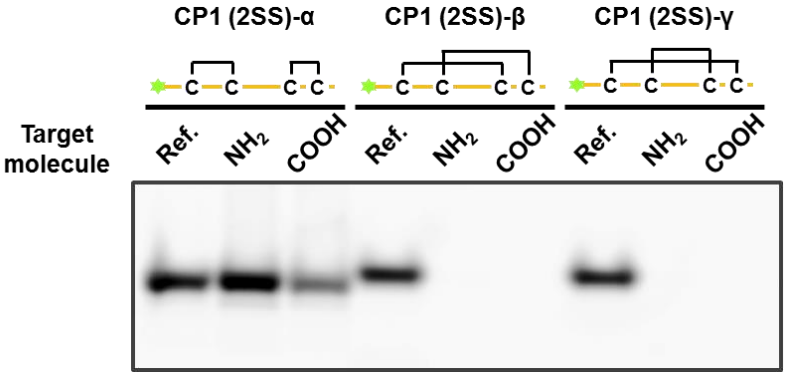

Figure 3–5. Binding assay of the disulfide isomers of CP1 (2SS): CP1 (2SS)-α, β, and γ against amino groups or carboxyl groups by a pull-down assay. Each disulfide isomer of CP1 (2SS) was incubated with amino group (NH_2) or carboxyl group (COOH) modified magnetic beads at 25 °C for 2 h in a selection buffer (20 mM Tris-HCl, pH 7.4, 1 M NaCl, 1 mM EDTA, 0.1% Tween-20). After washing the beads, the remaining CP1 was eluted with SDS sample buffer. The eluates were subjected to Tricine-SDS-PAGE and visualized with a fluorescence image analyser. A sample (3.3%) of each imputed disulfide isomer of CP1 (2SS) was loaded as a reference (Lane: Ref.).

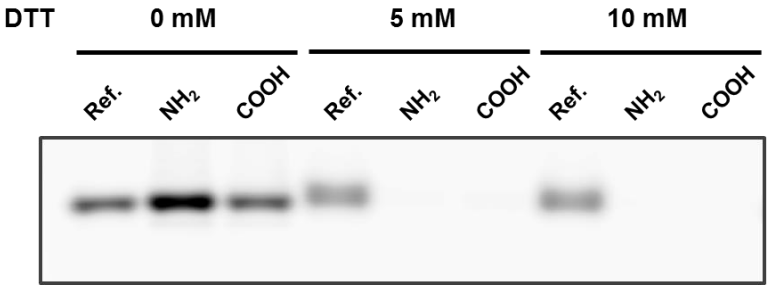

Figure 3–6. Pull-down assay of CP1 (2SS)-α under reduced conditions. CP1 (2SS)-α was pull-downed with amino group modified magnetic beads or carboxyl group modified magnetic beads under several concentrations of DTT (0–10 mM). Each eluate was analyzed by Tricine-SDS-PAGE and visualized by the Fluoroimager. A sample (3.3%) of each imputed CP1 (2SS)-α under each condition was loaded as a reference (Lane: Ref.).

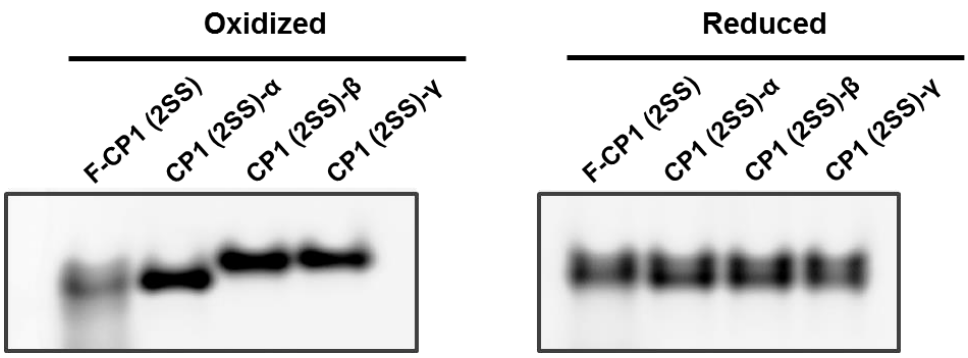

Figure 3–7. Mobility comparison of disulfide isomers of CP1 (2SS) on Tricine-SDS-PAGE. Four peptides: Fluorescein-labeled CP1 (2SS), three kinds of disulfide isomers of CP1 (2SS) were treated with 2-mercaptoethanol (right) or not (left) and subjected to Tricine-SDS-APGE. Tricine-SDS-PAGE gel was visualized by the Fluoroimager.

3-3-4. Binding assay against amino groups on several kinds of solid supports

To clear that the CP1 (2SS)-α interact with not material of the magnetic beads but amino group (NH_2) on the beads, binding assay against other solid supports (glass slide and agarose beads) was performed. We found that CP1 (2SS)-α was the most remained on the glass slide after washing with the selection buffer for 1 hr (Figure 3–8A). In addition, we found that more amount of CP1 (2SS)-α remained on the agarose beads after washing with the selection buffer compared with other two disulfide isomers of CP1 (2SS) and alanine variant of CP1 (Figure 3–8B). These results were consistent with the result of pull-down assay (Figure 3–3, Figure 3–5). These shows that the CP1 (2SS)-α can interact to amino group on each supports but not surfaces of each supports (magnetic beads, glass slide, or agarose beads).

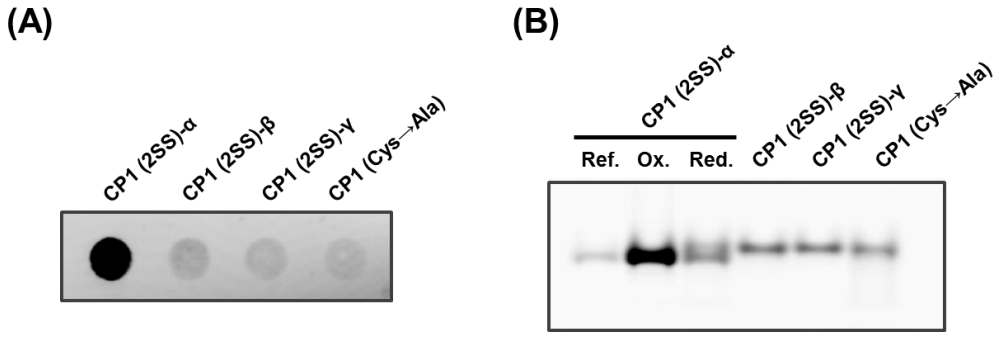

Figure 3-8. Binding assay of CP1 (2SS)-α against amino groups on several types of support. (A) The three disulfide isomers of CP1 (2SS) and CP1 (Cys→Ala) were spotted on an amino-group modified glass slide and each peptide remaining on the glass slide after washing was visualized with a fluorescence image analyser. (B) The three disulfide isomers of CP1 and CP1 (Cys→Ala) were incubated with amino-group modified agarose-resin beads. CP1-1 (2SS)-α was incubated with the agarose-resin beads under oxidizing conditions (Ox.) or reducing conditions with DTT (Red.). After washing the agarose-resin beads, each remaining peptide was eluted with SDS sample buffer. Each eluate was subjected to Tricine-SDS-PAGE and visualized with the Fluoroimager. CP1 (2SS)-α (1 pmol) was loaded as a reference (Lane: Ref.).

3-3-5. Binding assay of CP1 (2SS)-α derivative peptides

In previous studies, many kinds of cyclic peptides containing a disulfide bond have been developed to achieve high affinity and specificity against proteins. Although CP1 (2SS)-α contains two disulfide-bridged loops, it is uncertain whether both these constrained cyclic loops are indispensable for recognition of the amino group. Hence, to investigate whether both loops are required for recognition, all possible combinatorial pattern peptides of CP1 (2SS)-α which have only a single cyclic loop, with or without each remaining region in which cysteines were substituted to serines, were chemically synthesized (Table 3–3). According to a binding assay of these peptides

against amino groups on magnetic beads, only CP1 (2SS)-α could recognize the amino group (Figure 3–9). This indicates that both cyclic loops in the peptide CP1 (2SS)-α are required for amino group recognition. Moreover, the flexible region between the cyclic loops may also be required for molecular recognition.

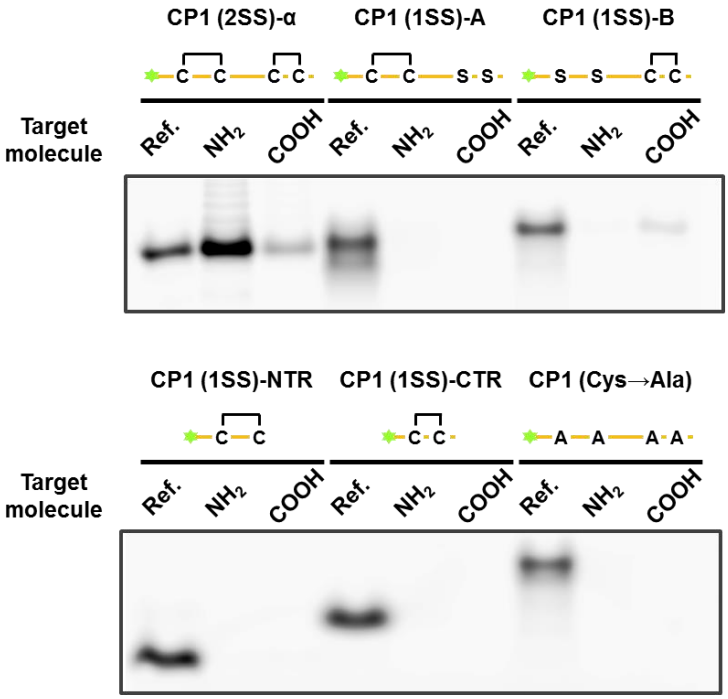

Figure 3-9. Binding assay of CP1 (2SS) derivative peptides. CP1 (2SS)-α and five derivative peptides of CP1 (2SS)-α: CP1 (1SS)-A, CP1 (1SS)-B, CP1 (1SS)-NTR, CP1 (1SS)-CTR, and CP1 (Cys→Ala) were assayed by the pull-down method under the conditions as described for Figure 3–6. A sample (3.3%) of each imputed CP1 (2SS) derivative peptide was loaded as a reference (Lane: Ref.).

3-3-6. Secondary structure analysis

In a previous study, we found that a peptide with two disulfide bridges interacts with the interleukin 6 receptor (IL-6R) with high affinity and specificity [51,77]. However, the disulfide connectivity in this peptide is similar to CP1 (2SS)-γ, which is different to CP1 (2SS)-α. The disulfide bridges in CP1 (2SS)-γ causes the molecule to become rigid, but CP1 (2SS)-α, with two cyclic loops, can has both rigid and flexible regions. Circular dichroism (CD) spectroscopy results showed that CP1 (2SS)-α contained secondary structures, although CP1 (Cys→Ala) was in a random coil state (Figure 3–10). This result suggests that the disulfide bonds might enable the peptide to form secondary structures. In a previous study on polymer-binding peptides (7-mers) that recognize poly(methyl methacrylate), it was suggested that the rigid and kinked structure formed by proline and possible hairpin conformation of the essential 4-mer sequence is the most important aspect for peptide affinity [78]. Recently, the same authors reported the screening, by *in vitro* selection using phage display, of short 12-mer peptides recognizing the simplest polycyclic aromatic hydrocarbon, naphthalene; both the phenylalanine and proline residues were shown to be essential for creating the specific affinity [79]. A rigid steric conformation for peptides may be very important for molecular recognition by improving the ability of the peptide to interact with a molecule.

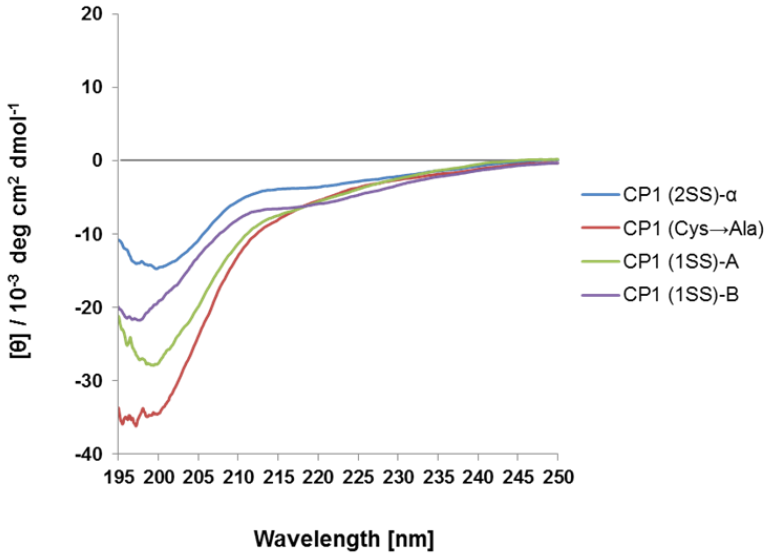

Figure 3–10. Circular dichroism analyses of CP1 derivative peptides. Each peptide concentration was 0.2 mg/mL in 20 mM sodium phosphate buffer, pH 7.4. The temperature was set at 25 °C.

3-4. Conclusions

We have demonstrated that 30-residue peptides containing two disulfide bridges recognize amino groups on a solid-phase and can be screened in an *in vitro* selection manner by cDNA display from a cysteine-rich peptide coding DNA library. Pull-down assays of the disulfide isomers of CP1 (2SS) showed that the unique disulfide bridge pattern of the CP1 (2SS)-α peptide is required for amino group recognition. Neither of the single cyclic loop regions of the CP1 (2SS)-α peptide could bind amino groups on the solid-phase. Interestingly, not only both cyclic loops, but also the linkage region between the loops is indispensable for recognition of the amino group. Therefore, the CP1 (2SS)-α peptide containing two cyclic loops with disulfide bonds forms a unique conformation that is able to bind the amino group. This study demonstrates that peptides containing disulfide bridges can recognize functional groups of organic molecules, such as amino groups. Constrained peptides containing disulfide bridges as described in this work may represent a new approach in the molecular recognition of small molecules.

4. Overall conclusions

First, we have established an *in vitro* selection/evolution system by cDNA display, which is suitable to use in the design of disulfide-rich peptide aptamers. Second, we have selected a disulfide-rich peptide aptamer recognizing amino groups on a solid phase. This is the first report of a disulfide-rich peptide aptamer recognizing a specific functional group. This study suggests that the limit of molecular recognition by peptides can be extended by introducing several patterns of disulfide bridges into the peptide. In addition, it was shown that the cDNA display method represents a powerful method to screen disulfide-rich peptides from a cysteine-rich peptide library.

References

1. Chan A.C. and Carter P.J. (2010) Therapeutic antibodies for autoimmunity and inflammation. *Nat. Rev. Immunol.*, **10**, 301-316.

2. Scott A.M., Wolchok J.D., and Old L.J. (2012) Antibody therapy of cancer. *Nat. Rev. Cancer*, **12**, 278-287.

3. Wurch T., Pierré A., and Depil S. (2012) Novel protein scaffolds as emerging therapeutic proteins: from discovery to clinical proof-of-concept. *Trends Biotechnol.*, **30**, 575-582.

4. Hosse R.J, Rothe A., and Power B.E. (2006) A new generation of protein display scaffolds for molecular recognition. *Protein Sci.*, **15**, 14-27.

5. Umetsu M., Nakanishi T., Asano R., Hattori T., and Kumagai I. (2010) Protein-protein interactions and selection: generation of molecule-binding proteins on the basis of tertiary structural information. *FEBS J.*, **277**, 2006-2014.

6. Zoller F., Haberkorn U., and Mier W. (2011) Miniproteins as phage display-scaffolds for clinical applications. *Molecules*, **16**, 2467-2485.

7. Hoppe-Seyler F., Crnkovic-Mertens I., Tomai E., and Butz K., (2004) Peptide Aptamers: Specific Inhibitors of Protein Function. *Curr. Mol. Med.*, **4**, 529-538.

8. Colas P. (2008) The eleven-year switch of peptide aptamers. *J. Biol.*, **7**, 2.

9. Colas P., Cohen B., Jessen T., Grishina I., McCoy J., and Brent R. (1996) Genetic selection of peptide aptamers that recognize and inhibit cyclin-dependent kinase 2. *Nature*, **380**. 548-550.

10. Liu M., Tada S., Ito M., Abe H., and Ito Y. (2012) In vitro selection of a photo-responsive peptide aptamer using ribosome display. *Chem. Commun.*, **48**, 11871-11873.

11. Wada A. (2013) Development of Next-Generation Peptide Binders Using In vitro Display Technologies and Their Potential Applications. *Front Immunol.*, **4**, 224.

12. Shrivastava A., von Wronski M.A., Sato A.K., Dransfield D.T., Sexton D., Bogdan N., Pillai R., Nanjappan P., Song B., Marinelli E., DeOliveira D., Luneau C., Devlin M., Muruganandam A., Abujoub A., Connelly G., Wu Q.L., Conley G., Chang Q., Tweedle M.F., Ladner R.C., Swenson R.E., and Nunn A.D. (2005) A distinct strategy to generate high-affinity peptide binders to receptor tyrosine kinases. *Protein Eng. Des. Sel.*, **18**, 417-424.

13. Wilson A.J. (2009) Inhibition of protein–protein interactions using designed molecules. *Chem. Soc. Rev.*, **38**, 3289-3300.

14. Tamerler C. and Sarikaya M. (2009) Molecular biomimetics: nanotechnology and bionanotechnology using genetically engineered peptides. *Philos. Trans. A. Math. Phys. Eng. Sci.*, **367**, 1705-1726.

15. Lewis R.J. and Garcia M.L. (2003) Therapeutic potential of venom peptides. *Nat. Rev. Drug Discov.*, **10**, 790-802.

16. Antosova Z., Mackova M., Kral V., and Macek T. (2009) Therapeutic application of peptides and proteins: parenteral forever? *Trends Biotechnol.*, **11**, 628-635.

17. Góngora-Benítez M., Tulla-Puche J., and Albericio F. (2013) Multifaceted Roles of Disulfide Bonds. Peptides as Therapeutics. *Chem. Rev.*, DOI: 10.1021/cr400031z.

18. Shiba K. (2010) Natural and artificial peptide motifs: their origins and the application of motif-programming. *Chem. Soc. Rev.*, **39**, 117-126.

19. Seker U.O.S. and Demir H.V. (2011) Material binding peptides for nanotechnology. *Molecules*, **16**, 1426-1451.

20. Sawada T., Mihara H., and Serizawa T. (2013) Peptides as new smart bionanomaterials: molecular-recognition and self-assembly capabilities. *Chem. Rec.*, **13**, 172-186.

21. Angelini A. and Heinis C. (2011) Post-translational modification of genetically encoded polypeptide libraries. *Curr. Opin. Chem. Biol.*, **15**, 355-361.

22. Pasqualini R., Koivunen E., and Ruoslahti E. (1995) A peptide isolated from phage display libraries is a structural and functional mimic of an RGD-binding site on integrins. *J. Cell Biol.*, **130**, 1189-1196.

23. Wrighton N.C., Farrell F.X., Chang R., Kashyap A.K., Barbone F.P., Mulcahy L.S., Johnson D.L., Barrett R.W., Jolliffe L.K., and Dower W.J. (1996) Small peptides as potent mimetics of the protein hormone erythropoietin. *Science*, **273**, 458–464.

24. Heinis C., Rutherford T., Freund S., and Winter G. (2009) Phage-encoded combinatorial chemical libraries based on bicyclic peptides. *Nat. Chem. Biol.*, **5**, 502-507.

25. Hipolito C.J. and Suga H. (2012) Ribosomal production and in vitro selection of natural product-like peptidomimetics: the FIT and RaPID systems. *Curr. Opin. Chem. Biol.*, **16**, 196-203.

26. Ladner R.C. (1995) Constrained peptides as binding entities. *Trends Biotechnol.*, **13**, 426-430.

27. Chang H.J., Hsu H.J., Chang C.F., Peng H.P., Sun Y.K., Yu H.M., Shih H.C., Song C.Y., Lin Y.T., Chen C.C., Wang C.H., and Yang A.S. (2009) Molecular evolution of cystine-stabilized miniproteins as stable proteinaceous binders. *Structure*, **17**, 620-631.

28. Cemazar M., Kwon S., Mahatmanto T., Ravipati A.S., and Craik D.J. (2012) Discovery and applications of disulfide-rich cyclic peptides. *Curr. Top Med. Chem.*, **12**, 1534-1545.

29. Kolmar H. (2008) Alternative binding proteins: biological activity and therapeutic potential of cystine-knot miniproteins. *FEBS J.*, **275**, 2684-2690.

30. Kolmar H. (2009) Biological diversity and therapeutic potential of natural and engineered cystine knot miniproteins. *Curr. Opin. Pharmacol.*, **9**, 608-614.

31. Daly N.L. and Craik D.J. (2011) Bioactive cystine knot proteins. *Curr. Opin. Chem. Biol.*, **15**, 362-368.

32. Werle M., Kafedjiiski K., Kolmar H., and Bernkop-Schnurch A. (2007) Evaluation and improvement of the properties of the novel cystine-knot microprotein McoEeTI for oral administration. *Int. J. Pharm.*, **332**, 72-79.

33. Heitz A., Avrutina O., Le-Nguyen D., Diederichsen U., Hernandez J.F., Gracy J., Kolmar H., and Chiche L. (2008) Knottin cyclization: impact on structure and dynamics. *BMC Struct. Biol.*, **8**, 54.

34. Craik D.J., Daly N.L., and Waine C. (2001) The cystine knot motif in toxins and implications for drug design. *Toxicon*, **39**, 43-60.

35. Werle M., Schmitz T., Huang H.L., Wentzel A., Kolmar H., and Bernkop-Schnürch A. (2006) The potential of cystine-knot microproteins as novel pharmacophoric scaffolds in oral peptide drug delivery. *J. Drug Target*, **14**, 137-146.

36. Daly N.L. and Craik D.J. (2009) Structural studies of conotoxins. *IUBMB Life*, **61**, 144-150.

37. Norton R.S. and Olivera B.M. (2006) Conotoxins down under. *Toxicon*, **48**, 780-98.

38. Prommer E. (2006) Ziconotide: a new option for refractory pain. *Drugs Today*, **42**, 369–378.

39. Moore S.J., Leung C.L., and Cochran J.R. (2012) Knottins: disulfide-bonded therapeutic and diagnostic peptides. *Drug Discov. Today Technol.*, **9**, e1-e70.

40. Kolmar H. (2010) Engineered cystine-knot miniproteins for diagnostic applications. *Expert Rev. Mol. Diagn.*, **10**, 361-368.

41. Kimura R.H., Cheng Z., Gambhir S.S., and Cochran J.R. (2009) Engineered knottin peptides: a new class of agents for imaging integrin expression in living subjects. *Cancer Res.*, **69**, 2435-2442.

42. Kini R.M. (2011) Evolution of Three-Finger Toxins - a Versatile Mini Protein Scaffold. *Acta. Chim. Slov.*, **58**, 693-701.

43. Diochot S., Baron A., Salinas M., Douguet D., Scarzello S., Dabert-Gay A.S., Debayle D., Friend V., Alloui A., Lazdunski M., and Lingueglia E. (2012) Black mamba venom peptides target acid-sensing ion channels to abolish pain. *Nature*, **490**, 552-555.

44. Matsuura T. and Yomo T. (2006) In vitro evolution of proteins. *J. Biosci. Bioeng.*, **101**, 449-456.

45. Grönwall C. and Ståhl S. (2009) Engineered affinity proteins--generation and applications. *J. Biotechnol.*, **140**. 254-269.

46. Glökler J., Schütze T., and Konthur Z. (2010) Automation in the high-throughput selection of random combinatorial libraries--different approaches for select applications. *Molecules*, **15**, 2478-2490.

47. Takahashi T.T., Austin R.J., and Roberts R.W. (2003) mRNA display: ligand discovery, interaction analysis and beyond. *Trends Biochem. Sci.*, **28**, 159-165.

48. Nemoto N., Miyamoto-Sato E., Husimi Y., and Yanagawa H. (1997) In vitro virus: bonding of mRNA bearing puromycin at the 3'-terminal end to the C-terminal end of its encoded protein on the ribosome in vitro. *FEBS Lett.*, **414**, 405-408.

49. Roberts, R.W. and Szostak, J.W. (1997) RNA-peptide fusions for the in vitro selection of peptides and proteins. *Proc. Natl. Acad. Sci. USA*, **94**, 12297-12302.

50. Mattheakis, L.C., Bhatt, R.R. and Dower, W.J. (1994) An in vitro polysome display system for identifying ligands from very large peptide libraries. *Proc. Natl. Acad. Sci. USA*, **91**, 9022-9026.

51. Yamaguchi J., Naimuddin M., Biyani M., Sasaki T., Machida M., Kubo T., Funatsu T., Husimi Y., and Nemoto N. (2009) cDNA display: a novel screening method for functional disulfide-rich peptides by solid-phase synthesis and stabilization of mRNA-protein fusions. *Nucleic Acids Res.*, **37**, e108.

52. Ueno S. and Nemoto N. (2012) cDNA display: rapid stabilization of mRNA display. *Methods Mol. Biol.*, **805**, 113-135.

53. Kitamura K., Yoshida C., Kinoshita Y., Kadowaki T., Takahashi Y., Tayama T., Kawakubo T., Naimuddin M., Salimullah M., Nemoto N., Hanada K., Husimi Y., Yamamoto K., Nishigaki K. (2009) Development of systemic in vitro evolution and its application to generation of peptide-aptamer-based inhibitors of cathepsin E. *J. Mol. Biol.*, **387**, 1186-1198.

54. Mochizuki Y., Biyani M., Tsuji-Ueno S., Suzuki M., Nishigaki K., Husimi Y., and Nemoto N. (2011) One-pot preparation of mRNA/cDNA display by a novel and versatile puromycin-linker DNA. *ACS Comb. Sci.*, **13**, 478-485.

55. Ueno S., Kimura S., Ichiki T., and Nemoto N. (2012) Improvement of a puromycin-linker to extend the selection target varieties in cDNA display method. *J. Biotechnol.*, **162**, 299-302.

56. Naimuddin M., Kobayashi S., Tsutsui C., Machida M., Nemoto N., Sakai T., and Kubo T. (2011) Directed evolution of a three-finger neurotoxin by using cDNA display yields antagonists as well as agonists of interleukin-6 receptor signaling. *Mol. Brain*, **4**, 2.

57. Ueno S., Yoshida S., Mondal A., Nishina K., Koyama M., Sakata I., Miura K., Hayashi Y., Nemoto N., Nishigaki K., and Sakai T. (2012) In vitro selection of a peptide antagonist of growth hormone secretagogue receptor using cDNA display. *Proc. Natl. Acad. Sci. USA*, **109,** 11121-11126.

58. Tsuji-Ueno S., Komatsu M., Iguchi K., Takahashi M., Yoshino S., Suzuki M., Nemoto N., and Nishigaki K. (2011) Novel high-affinity Aβ-binding peptides identified by an advanced in vitro evolution, progressive library method. *Protein Pept. Lett.*, **18**, 642-650.

59. Chen S., Rentero Rebollo I., Buth S.A., Morales-Sanfrutos J., Touati J., Leiman P.G., and Heinis C. (2013) Bicyclic peptide ligands pulled out of cysteine-rich peptide libraries. *J. Am. Chem. Soc.*, **135**, 6562-6569.

60. Singh R. (2008) A review of algorithmic techniques for disulfide-bond determination. *Brief Funct. Genomic. Proteomic.*, **7**, 157-172.

61. Nemoto N., Miyamoto-Sato E., and Yanagawa H. (1999) Fluorescein labeling of the C-terminus of proteins with a puromycin analogue in cell-free translation systems. *FEBS Lett.*, **462**, 43–46.

62. Wegner G.J., Lee H.J., and Corn R.M. (2002) Characterization and optimization of peptide arrays for the study of epitope–antibody interactions using surface plasmon resonance imaging. *Anal. Chem.*, **74**, 5161–5168.

63. Anti-mouse Fas Ligand/CD178, Data Sheet D069–3. MBL International, Woburn, MA, 2008.

64. Binding Characteristics of protein A, protein G, protein A/G and protein L, Technical Resource, Thermo Fisher Scientific, Rockford, IL, 2004, TR0034.1.

65. Brymora A., Cousin M.A., Roufogalis B.D., and Robinson P.J. (2001) Enhanced protein recovery and reproducibility from pull-down assays and immunoprecipitations using spin columns. *Anal. Biochem.*, **295**, 119–122.

66. Ren L., Chang E., Makky K., Haas A.L, Kaboord B., and Qoronfleh M.W. (2003) Glutathione S-transferase pull-down assays using dehydrated immobilized glutathione resin. *Anal. Biochem.*, **322**, 164–169.

67. Suzuki H., Ogawa C., Usui K., and Hayashizaki Y. (2004) In vitro pull-down assay without expression constructs. *BioTechniques*, **37**, 918–920.

68. Hassert R. and Beck-Sickinger A.G. (2013) Tuning peptide affinity for biofunctionalized surfaces. *Eur. J. Pharm. Biopharm.*, **85**, 69-77.

69. Saggio I. and Laufer R. (1993) Biotin binders selected from a random peptide library expressed on phage. *Biochem. J.*, **293**, 613-616.

70. Rozinov M.N. and Nolan G.P. (1998) Evolution of peptides that modulate the spectral qualities of bound, small-molecule fluorophores. *Chem. Biol.*, **5**, 713-728.

71. Marks K.M., Rosinov M., and Nolan G.P. (2004) In vivo targeting of organic calcium sensors via genetically selected peptides. *Chem Biol.*, **11**. 347-356.

72. Wang W., Hara S., Liu M., Aigaki T., Shimizu S., and Ito Y. (2011) Polypeptide aptamer selection using a stabilized ribosome display. *J. Biosci. Bioeng.*, **112**, 515-517.

73. Kühl T., Sahoo N., Nikolajski M., Schlott B., Heinemann S.H., and Imhof D. (2011) Determination of hemin-binding characteristics of proteins by a combinatorial peptide library approach. *Chembiochem.*, **12**, 2846-2855.

74. Baeriswyl V. and Heinis C. (2013) Polycyclic peptide therapeutics. *ChemMedChem*, **8**, 377-384.

75. Ceroni A., Passerini A., Vullo A., and Frasconi P. (2006) DISULFIND: a disulfide bonding state and cysteine connectivity prediction server. *Nucleic Acids Res.*, **34**, W177-W181.

76. Steiner A.M., Woycechowsky K.J., Olivera B.M., and Bulaj G. (2012) Reagentless oxidative folding of disulfide-rich peptides catalyzed by an intramolecular diselenide. *Angew. Chem. Int. Ed. Engl.*, **51**, 5580-5584.

77. Nemoto N., Tsutsui C., Yamaguchi J., Ueno S., Machida M., Kobayashi T., and Sakai T. (2012) Antagonistic effect of disulfide-rich peptide aptamers selected by cDNA display on interleukin-6-dependent cell proliferation. *Biochem. Biophys. Res. Commun.*, 2012, **421**, 129-133.

78. Serizawa T., Sawada T., and Matsuno H. (2007) Highly Specific Affinities of Short Peptides against Synthetic Polymers., *Langmuir*, **23**, 11127-11133.

79. Sawada T., Okeya Y., Hashizume M., and Serizawa T. (2013) Screening of Peptides Recognizing Simple Polycyclic Aromatic Hydrocarbons. *Chem. Commun.*, **49**, 5088-5090.

Acknowledgments

First of all, I would like to express my deepest and sincere gratitude to my supervisor Prof. Naoto Nemoto for many educations which are needed to become a scientist. I have been really influenced by his attitude towards science. He had taught me basic, essential, and important insight for scientist. I learned how to think, how to conduct research study, how to design experiments, how to resolve problems, how to perform presentations, how to write papers, and how to enjoy science. In addition, we thank him to give me a very interesting theme for me and providing an excellent environment for the experiments.

I thank sub-supervisor Prof. Koichi Nishigaki at Saitama University for supervising of this study and teaching basic attitude of scientist. I thank Assist. Prof. Miho Suzuki for technical advices and teaching English presentation and writing. I thank Dr. Shingo Ueno who has been giving insightful technical advises and discussion. I thank Dr. Tetsuo Koyama and Mr. Niimi Tomohisa for help with TOF-MS analysis. I'm grateful to Assist. Prof. Hisashi Tadakuma at University of Tokyo and Dr. Yusuke Maeda at Tokyo University of Science for help with CD measurement.

I thank other laboratory members of Nemoto laboratory and Nishigaki laboratory at Saitama University for stimulation, discussion, encouragements, and everything.

I thank all the scientists who are not mentioned here but interacted with me.

Lastly, I'm grateful for my families for supports to devote my life to study.